CZECH TECHNICAL UNIVERSITY IN PRAGUE

FACULTY OF CIVIL ENGINEERING

Analysis of Composite Structures

by

Natalino Gattesco

Associate Professor CTU Prague

Prague, September 2011

Summary

The main aspects that have to be considered in the analysis of composite structures are presented and discussed. Most of composite structures concern floors of buildings and bridges, so that in this lecture the attention is mainly devoted to composite beams.

To correctly evaluate stresses in the concrete slab an effective width is considered to account for shear lag and moreover, to account for local buckling phenomena, the sections are divided in four classes according to the slenderness of the parts in compression. The moment of resistance of sections is calculated through plastic analysis in sections belonging to class 1 or 2, whereas the elastic analysis is used for sections in class 3 or 4. In case of plastic analysis a partial shear connection may be provided in sagging moment regions; in this case the section moment of resistance is governed by the resistance of the shear connection.

In the elastic analysis of sections the effects of creep and shrinkage have to be considered because they cause significant redistribution of section stresses. At serviceability limit states, besides the check on the values of stresses, the deflection and the crack width need to be limited. The tension stiffening of concrete in tension among two consecutive cracks needs to be considered to evaluate correctly the deflection in continuous composite beams.

The global analysis may be carried out using elastic analysis. At ultimate limit state some moment redistribution to account for the inelastic behavior of materials and for cracking has to be applied to optimize the sections. The limits of moment redistribution are related to the maximum rotation capacity of the sections subjected to maximum hogging moments.

A broad numerical study was carried out by the author to determine the permissible moment redistribution domain that satisfies at the same time both the rotation compatibility and the crack width in service. Propped cantilevers and fixed-end beams with different types of class 1 sections were considered in the study. Moreover a low ductility reinforcing steel (elongation at maximum load 2.5%) was considered. The results of the study allowed to provide a proposal for new moment redistribution limits.

A numerical procedure able to analyze the structural behavior of steel-concrete composite beams subjected to very heavy moving loads, considering the actual cyclic nonlinear relationship between the shear force and the slip of the connectors, was also developed by the author. The procedure allowed determining the oscillograms of the slip and the shear force of each connector corresponding to the transit of an assigned loading pattern. Fatigue checks, based on the strain-life approach can be carried out using such a numerical tool. The results of a numerical study of a 40 m span simply supported bridge-type beam subjected to very heavy low frequent vehicles allowed to assess the damage accumulated in the connectors due to one thousand transits of the considered load. Significant damage was found in the studs close to mid-span.

Souhrn

Jsou prezentovány a diskutovány hlavní aspekty, které je třeba respektovat při analýze kompozitních konstrukcí. Většina kompozitních konstrukcí nachází uplatnění v podlahových a mostních konstrukcích, a proto se přednáška zaměřuje na spřažené nosníky.

Pro výstižný popis napjatosti je nutno vzít v úvahu nejen účinky ochabnutí smykem v betonové desce (spolupůsobící šířky), ale též jevy místního boulení - průřezy jsou pro tlakové působení podle štíhlosti jejich částí děleny do čtyř tříd. Moment odporu se počítá použitím plastické analýzy v průřezech, které patří do třídy 1 nebo 2, pro části třídy 3 nebo 4 je používána elastická analýza. V případě plastické analýzy může být v oblastech kladných momentů uvažováno částečné spřažení, v tomto případě je moment odporu průřezu dán odporem spřažení.

Při elastické analýze je třeba vzít v úvahu účinky dotvarování a smršťování betonu, protože mohou způsobit významnou redistribuci napětí. V mezních stavech použitelnosti, kromě kontroly hodnot napětí, je nutno zajistit omezení deformací a šířky trhlin. Pro výstižné stanovení průhybů spřažených spojitých nosníků je v tahových oblastech nutno uvážit jev tahového zpevnění betonu mezi sousedními trhlinami.

Globální analýza může být provedena použitím elastického přístupu. Pro optimalizaci průřezů v mezním stavu je nutno respektovat redistribuci namáhání související s neelastickým chováním materiálů a vznikem trhlin. Míra redistribuce je omezena maximální rotační kapacitou průřezů namáhaných zápornými ohybovými momenty.

Pro určení přípustné oblasti redistribuce ohybových momentů provedl autor rozsáhlou numerickou studii, která splňuje současně jak limity rotační kompatibility, tak i šířky trhlin v provozním režimu. Ve studii byly sledovány konzoly a vetknuté nosníky s různými typy průřezů třídy 1; uvažována byla betonářská ocel s nízkou tažností (poměrné prodloužení při maximálním zatížení 2,5%). Výsledky studie mohou poskytnout podklady pro zpřesněný návrh nových mezí pro přerozdělování ohybových momentů.

Autor odvodil numerický postup pro analýzu působení ocelobetonových spřažených nosníků vystavených přesunům pohyblivých nadměrně těžkých zatížení, respektující cyklické nelineární vztahy mezi smykovými sílami a pokluzem konektorů. Postup umožňuje možnost stanovení oscilogramů pokluzu a smykové síly každého konektoru odpovídající příslušnému zatěžujícímu schématu. Tímto výpočetním nástrojem může být provedeno sledování únavových projevů. Výsledky numerické studie prostého nosníku o rozpětí 40 m vystaveného přejezdům extrémně těžkého vozidla s nízkou frekvencí výskytu poskytly možnost stanovení akumulace poškození ve spřahovacích prvcích po tisíci přejezdech – v oblasti středu rozpětí bylo identifikováno jejich významné poškození.

Keywords

Composite structures, reinforced concrete, steel structures, structural analysis, shear connection, creep and shrinkage, fatigue.

Klíčová slova

Kompozitní konstrukce, železový beton, ocelové konstrukce, výpočtová analýza, spřažení, dotvarování a smršťování, únava.

Table of Contents

1   Introduction

The steel-concrete composite system comprehends the structures obtained joining, through particular connection devices, steel members, with different shapes (steel profiles, plates, trusses, etc.), to reinforced or prestressed concrete slabs. Composite structures are economically favourable with respect to reinforced concrete structures because they request limited formworks and the assembling of members is quicker. With respect to steel structures a lower quantity of steel is requested and the cost of concrete elements, that frequently are however present, is appreciably lower than that of the minor steel used.

The most frequent use of the composite system is in the construction of floors in steel industrial or office buildings (Johnson 1994) and in the construction of bridges and viaducts (Johnson & Buckby 1994). In some cases, the composite system is also used for the columns of buildings (Johnson 1994, Dezi & Gattesco 2006).

Composite floors concern both steel beams connected with solid concrete slabs and steel beams connected with composite slabs, made with profiled steel sheeting (Fig. 1). In a first time the profiled steel sheetings were smooth and they were used as structurally non-participating formwork; the production of profiled steel sheetings with embossments allowed to consider them as structurally participating (composite slabs). In the last two decades a new floor system started to be used, that consists in welded non symmetric steel beams (lower flange wider than the upper one) supporting deep profiled metal sheeting on the lower flange (Fig. 2). This system, named slimfloor, allows limited depths of the floor with significant advantages on the height of the building, the costs to realize the curtain walls, the installation of heating-cooling plants (Dezi & Gattesco 2006).
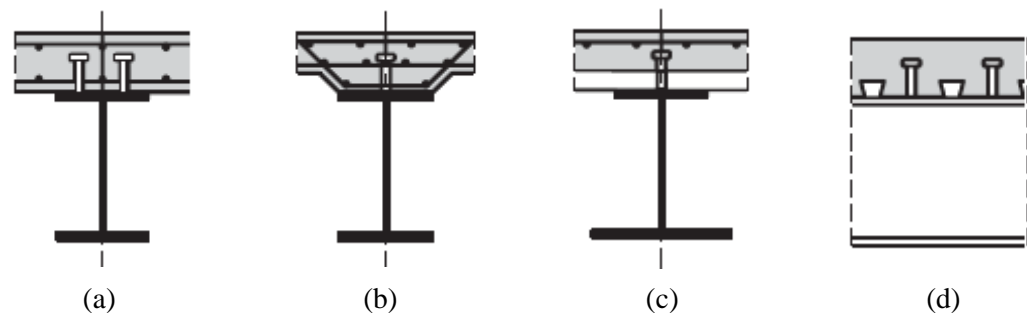

| (a) | (b) | (c) | (d) |

Figure 1 – Composite floors: (a,b) solid concrete slab, (c,d) profiled steel sheeting slab.

Figure 2 – Slimfloor system.

<div align="center">
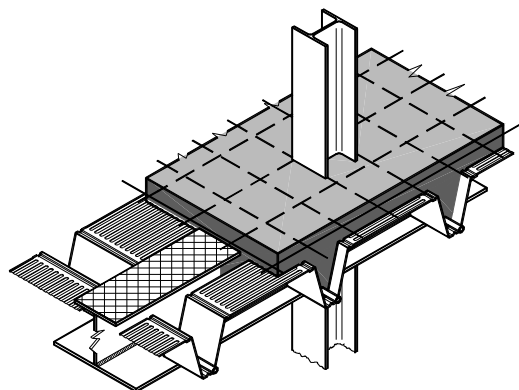
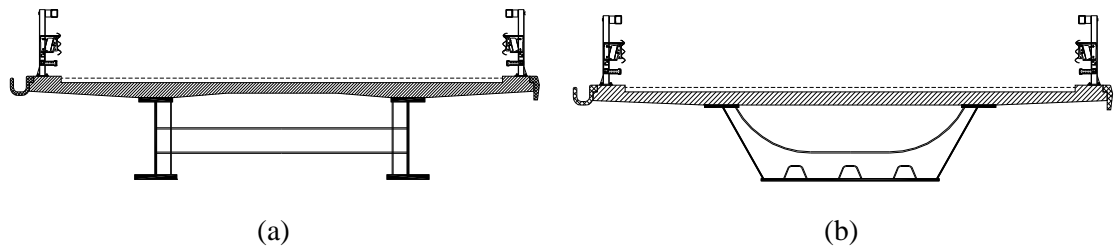(a)   (b)

Figure 3 – Composite bridges: (a) two parallel steel beams, (b) box girder.

</div>

A great part of bridges ranging from 30 m to 90 m span are made using the composite system (Dezi & Gattesco 2006). In the most part of composite bridges the steel member is formed either by a couple of parallel beams (Fig. 3a) or by a box girder (Fig. 3b). The first solution is the most used because it is easier to be constructed and economically more favourable. The latter becomes preferable when it is needed a great torsional stiffness, when the depth of the deck has to be limited and when a better aesthetic aspect is requested.

The behavior of the composite system is significantly different with respect to concrete structures and steel structures, because of the interaction of the two materials. This interaction emphasizes considerably the effects of time dependent phenomena because creep and shrinkage interest only the concrete; the steel, that is solidarized to the concrete, contrasts the deformation variations causing significant changes in the stress distribution (Gilbert & Bradford 1995, Macorini et al. 2006, Dezi et al. 1995).

The global analysis is frequently based on an elastic analysis which accounts for the actual nonlinear behavior (e.g. cracking, yielding of steel) through a redistribution of elastic moments. A deepen study is needed to calibrate the maximum allowable moment redistribution (Gattesco & Cohn 1989, Gattesco et al. 2010).

Moreover bridges are subjected to cyclic loads due to vehicle passages, so that the problem of fatigue has to be faced with great care (Dezi & Gattesco 2006, Gattesco & Pitacco 2004, Teraszkiewicz 1967).

In the present lecture the main aspects that characterize the flexural behavior of composite structures is detailed devoting special attention to the assessment of allowable moment redistribution and to the problem of low-cycle fatigue in the shear connection of bridges.

2   Shear connection

In most composite beams the concrete member is cast over the steel element and so a natural bond develops at their interface. But, this effect may be destroyed by shrinkage, poor adhesion, stresses due to variations of temperature, so it is necessary to provide adequate tools (shear connectors) to transfer effectively the longitudinal shear from the concrete to the steel member.

Many types of shear connectors for steel-concrete composite beams were developed in the last century, starting from the system proposed by Julius Kahn in 1903 (Fig. 4a), the spiral (Fig. 4b), the channel (Fig. 4c), the headed studs in 1956 (Fig. 4d), etc. However the development of the research on connection techniques was very low (e.g. Johnson 1994, Chapman & Balakrishnan 1964, Ollgart et al. 1971) so that the use of composite systems became diffuse also in building constructions only in the last three-four decades.

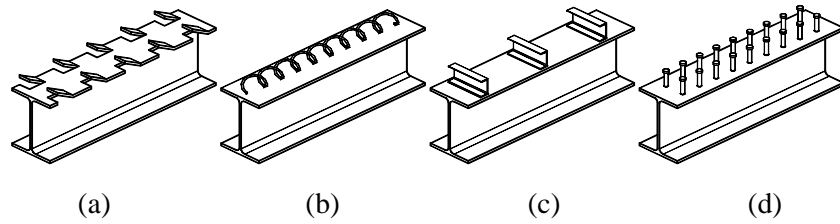(a)   (b)   (c)   (d)

Figure 4 – Connection systems for steel-concrete composite beams.

The most widely used type of connector is the headed stud (Fig. 4d). The range in diameter is from 13 to 25 mm. The studs are welded on the top flange of the steel beam. The shear capacity of studs is relatively low, so that a significant number of connectors is necessary. Stud connectors may be used to connect both solid slabs (Fig. 5a,b) and slabs made with profiled steel sheetings (Fig. 5c,d).

(a)   (b)   (c)   (d)
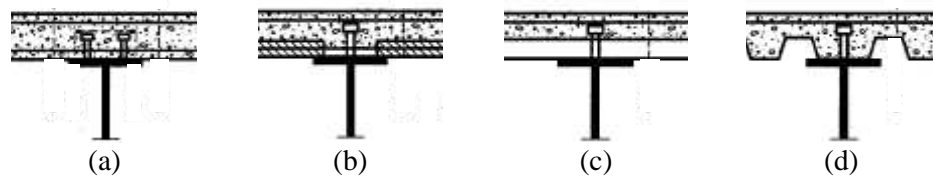
Figure 5 – Different applications of stud connectors in composite beams: a) solid slab, b) partly precast slab, c) slab with profiled steel sheeting perpendicular to steel joist and d) parallel to steel joist.

Other types of connectors used with solid slab are block connectors, made by welding parts of steel profiles (square, T-shaped, C-shaped, U-shaped, etc.) on the beam top flange (Fig. 6). This connection is characterized by very high stiffness. Also anchor and hoops are used as shear connectors in some cases coupled with square blocks.
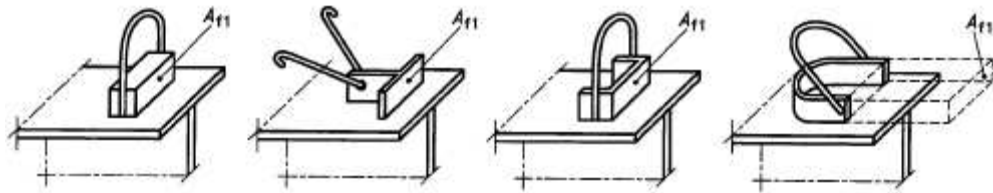
Figure 6 – Block connectors.

3 Characteristics of transversal sections

To proceed with the structural analysis of composite structures and their sections it is necessary to make some considerations about the characteristics of the sections.

3.1 Effective cross section

The longitudinal shear in the slab causes shear strains in its plane with the consequence that vertical cross sections of the composite T-beam do not remain plane, when subjected to bending moment. So that, at a cross section, the mean longitudinal stresses in the slab due to

bending moment varies along the flange breadth as illustrated in Fig. 7. The simple bending theory can give the correct maximum stress (point D) if the flange breadth *B* is replaced by an effective width, *b*, such that the area GHJK equals the area ACDEF. The results of the research on this concern, based on the elastic theory, has shown that the ratio *b/B* depends on the ratio *B/l*, the type of loading, the boundary conditions at the supports and other variables. However, for beams in buildings, it is enough accurate to assume that the effective width is equal to $l_o/8$ on each side of the steel web. The length l_o is the distance between points of zero bending moment. For simply supported beams this length is equal to the span. In case of continuous beams the lengths l_o suggested by most codes of practice are those illustrated in Fig. 8 (e.g. Eurocode 4 2004, Kristek et al. 1990).
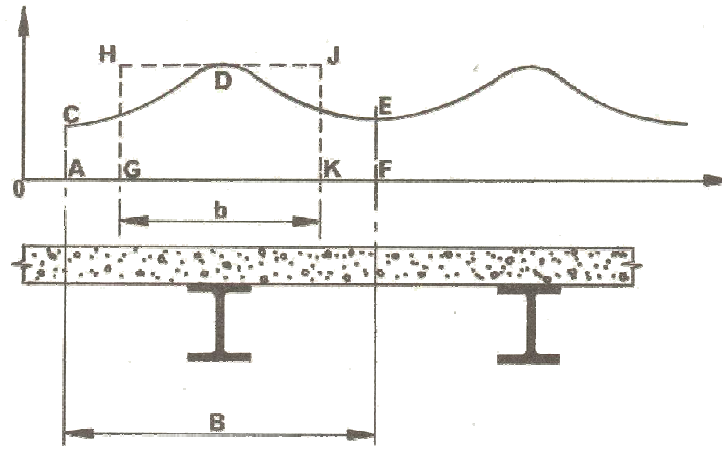
Figure 7 – Slab mean stress distribution due to shear lag and effective width.

1 $l_o= 0.85\, l_1$

2 $l_o= 0.25\, (l_1 + l_2)$

3 $l_o= 0.70\, l_2$

4 $l_o= 2\, l_3$
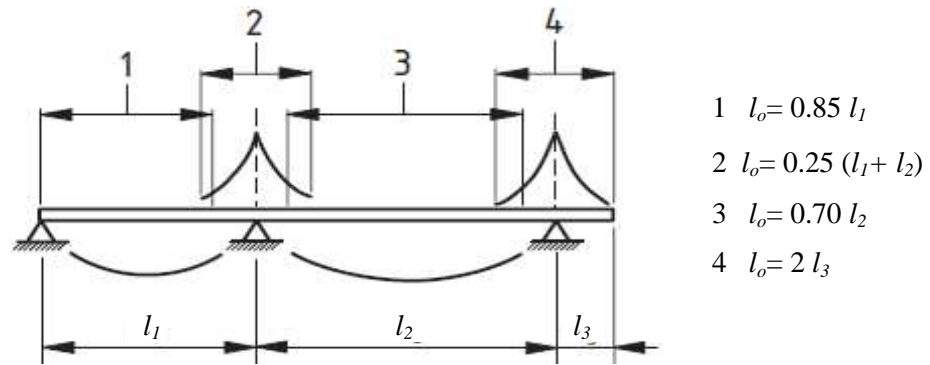
Figure 8 – Equivalent spans for effective width of concrete flange.
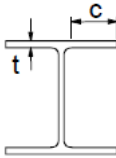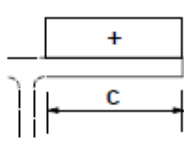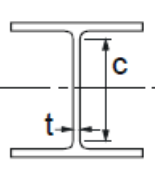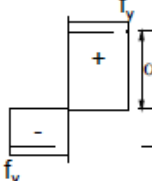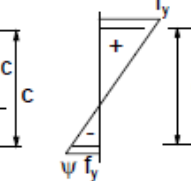
3.2   Classification of steel elements in compression

Due to the occurrence of local buckling, the resistance to compression of steel flanges or webs depends on their slenderness, represented by the breadth/thickness ratio (Kemp 1985). In many Codes of practice (e.g. Eurocode 4-2004, Eurocode 3-2005) each flange or web in compression is subdivided in four classes: 1) plastic, 2) compact, 3) semi-compact, 4) slender.

Class 1 cross sections are those which can form a plastic hinge with the rotation capacity required from plastic analysis without reduction of resistance. Class2 are those sections which can develop their plastic moment resistance, but have limited rotation capacity because of

local buckling. Class 3 are those sections in which in the extreme compression fiber of the steel member, assuming an elastic distribution of stresses, the yield strength can be reached, but local buckling is liable to prevent the development of the plastic moment resistance. Class 4 cross sections are those in which local buckling will occur before the attainment of the yield stress in one or more parts of the section.

Table 1 – Classification of sections.

Compression parts		Class 1	Class 2	Class 3
		c/t		
		9ε	10ε	14ε
		$\alpha > 0.5$ $\dfrac{396\,\varepsilon}{13\alpha-1}$ $\alpha \leq 0.5$ $\dfrac{36\,\varepsilon}{\alpha}$	$\alpha > 0.5$ $\dfrac{456\varepsilon}{13\alpha-1}$ $\alpha \leq 0.5$ $\dfrac{41.5\varepsilon}{\alpha}$	$\psi > -1$ $\dfrac{42\varepsilon}{0.67+0.33\psi}$ $\psi \leq -1$ $\dfrac{62\varepsilon(1-\psi)\sqrt{|\psi|}}{\alpha}$

$\varepsilon = \sqrt{235/f_y}$

The class of a cross section of a composite beam is the lower of the classes of its web and compression flange, and this class determines the design procedures that are available. If steel flanges are connected to a concrete slab they may be considered belonging to the Class 1. The slenderness ratios that define the limits among classes for steel flanges and webs are reported in Table 1.

The methods for the global analysis and for the analysis of cross section allowed are summarized according to the class of the section in Table 2. Elastic analysis may be used for all class sections, but in case of class 1 or 2 it is overconservative. The elastic analysis of sections in class 4 requests either to refer to a reduced yielding strength or to consider an effective width of the member, so to account for local buckling.

Table 2 – Methods of analysis according to section class.

Type of analysis	Class 1	Class 2	Class 3	Class 4
Global analysis	*plastic*	*elastic*	*elastic*	*elastic*
Section analysis	*plastic*	*plastic*	*elastic*	*elastic*

4 Ultimate resistance of sections to bending moment

As evidenced in Table 2, the analysis of sections in class 1 and 2 may be done with reference to both elastic or plastic analysis, whereas for sections in the other classes only the elastic analysis may be used. In case of plastic analysis the whole of the design load can be assumed to be resisted by the composite member, whether the construction was propped or unpropped.

This is because the inelastic behavior that precedes flexural failure allows internal redistribution of stresses to occur. On the contrary, the resistance to bending of beams with semi-compact or slender sections (class 3 or 4) is governed usually by the maximum stress in the steel section, calculated by elastic analysis. Account has to be taken of the construction method (propped, unpropped, prestressing systems, etc.) and of the creep and shrinkage. Actually, for sections with flanges in class 1 or 2 and the web in class 3 it is possible to use plastic analysis by neglecting a region in the center of the compressed part of the web, that is assumed to be ineffective because of buckling. The "hole-in-the-web" method is analogous to the use of effective widths for the design of steel compression elements in Class 4.

4.1   Cross sections in class 1 or 2

On consider one beam of a composite floor in which the slab is made with profiled steel sheeting. In section analysis the presence of the profiled steel sheeting is ignored when the slab is considered as part of the top flange of the composite beam. The main assumptions in section analysis are as follow:

- the tensile strength of concrete is neglected;
- plane cross sections of the structural steel and reinforced concrete parts of a composite section remain plane;
- rigid-plastic behavior for steel and concrete.

4.1.1   Resistance to sagging bending moment

There are three common situations: neutral axis within the concrete slab, neutral axis within the steel top flange and partial shear connection.

4.1.1.1   *Neutral axis within the concrete slab*

Considering the stress blocks shown in Fig. 9b, the depth x, assumed to be the position of the plastic neutral axis, is found by horizontal equilibrium:

$$N_{cf} = \frac{A_a f_y}{\gamma_a} = b_{eff}\, x \frac{0.85 f_{ck}}{\gamma_c}. \tag{1}$$
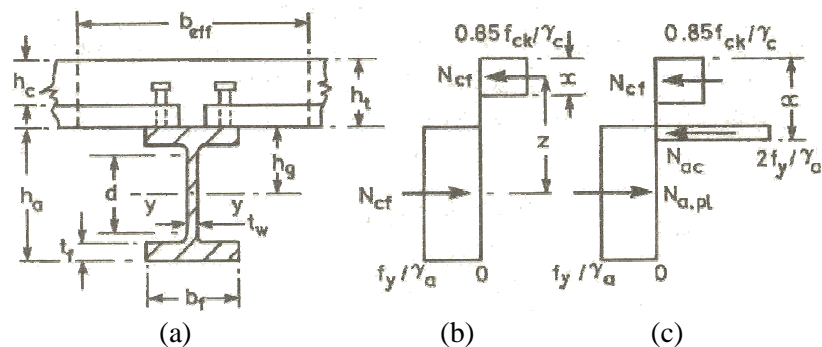

Figure 9 – Resistance to sagging bending of composite section (full shear connection).

From Eq. (1) on obtain

$$x = \frac{A_a\, f_y}{0.85\, f_{ck}\, b_{eff}} \cdot \frac{\gamma_c}{\gamma_a} \qquad (x \le h_c)\,. \tag{2}$$

The moments about the line of action of the force in the slab is

$$M_{pl,Rd} = \frac{A_a\, f_y}{\gamma_a} \cdot (h_g + h_t - \frac{x}{2})\,, \tag{3}$$

where h_g defines the position of the center of area of the steel section, with respect to the top flange of the profile.

4.1.1.2 *Neutral axis within the steel element*

Considering the stress blocks shown in Fig. 9c, the force N_{cf}, given by

$$N_{cf} = b_{eff}\, h_c\, \frac{0.85\, f_{ck}}{\gamma_c}\,, \tag{4}$$

is now less that the yield force for the steel section

$$N_{a,pl} = \frac{A_a\, f_y}{\gamma_a}\,, \tag{5}$$

so the neutral axis is at a depth $x > h_t$. The difference between the forces in Eqs. (4) and (5) is

$$N_{ac} = N_{a,pl} - N_{cf}\,. \tag{6}$$

If

$$N_{ac} \le 2 b_f\, t_f \cdot \frac{f_y}{\gamma_a} \tag{7}$$

the neutral axis lies within the steel top flange (Fig. 9c), and is equal to

$$N_{ac} = 2 b_f (x - h_t) \cdot \frac{f_y}{\gamma_a} \quad \Rightarrow \quad x = \frac{N_{ac} \cdot \gamma_a}{2 f_y\, b_f} + h_t\,. \tag{8}$$

The plastic moment is

$$M_{pl,Rd} = N_{a,pl} \cdot (h_g + h_t - \frac{h_c}{2}) - N_{ac}\, \frac{x - h_c + h_t}{2}\,. \tag{9}$$

If the inequality (7) is failed, the neutral axis lies within the steel web

$$N_{ac} = 2 b_f t_f \cdot \frac{f_y}{\gamma_a} + 2 t_w (x - h_t - t_f) \cdot \frac{f_y}{\gamma_a} \quad \Rightarrow \quad x = \frac{N_{ac} \cdot \gamma_a}{2 f_y\, t_w} - \frac{b_f\, t_f}{t_w} h_t + t_f\,. \tag{10}$$

The plastic moment may be then simply determined.

4.1.1.3 *Partial shear connection*

The force N_{cf} is the force that the shear connectors between the section of maximum sagging moment and a free end of the beam or the point of zero moment in case of continuous beams have to support (full shear connection). So the connection has to support a force at least equal to the minimum obtained through Eq. (1) and Eq. (4) $F_{cf} \ge N_{cf}$. If the shear connection is designed to resist a force F_c smaller than F_{cf} the flexural resistance of the beam is governed by the resistance of the connection (partial shear connection – Eurocode 4-2004). If each

connector has the same resistance to shear and the number in each shear span is N, then the degree of shear connection is defined by:

$$\frac{N}{N_f} = \frac{F_c}{F_{cf}} \tag{11}$$

where N_f is the number of connectors required for full shear connection.

The depth of the compressive stress block in the slab (Fig. 10) is obtained through horizontal equilibrium

$$x_c = \frac{F_c \, \gamma_c}{0.85 \, f_{ck} \, b_{eff}} \qquad (x_c \le h_c). \tag{12}$$

The distribution of longitudinal strains in the cross section is illustrated in Fig. 10b. The neutral axis in the slab is at a depth x_n greater than x_c ($x_c/x_n = \sim 0.8 \div 0.9$), but for simplicity they are assumed equal; the consequent error in the evaluation of the plastic moment is negligible.

There is a second neutral axis within the steel member. If it lies within the steel top flange, the stress blocks are as shown in Fig. 9c, but with a smaller resultant F_c instead of N_{cf}.

(a)   (b)   (c)
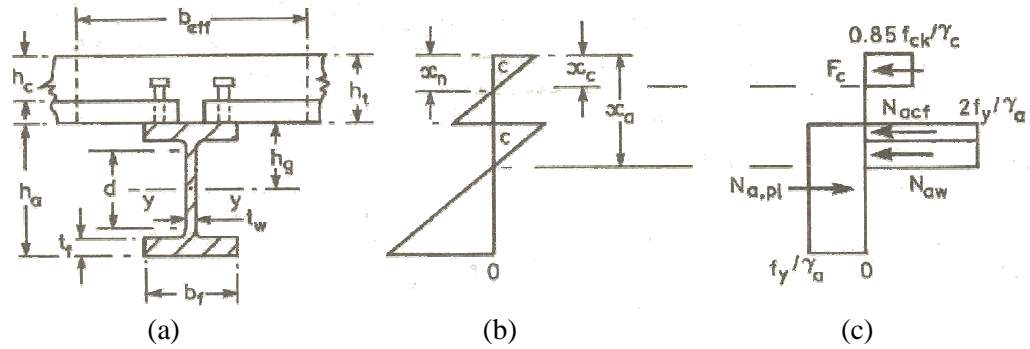
Figure 10 – Resistance to sagging bending of composite section (partial shear connection).

By analogy with equation (8), the neutral axis position is equal to

$$N_{a,pl} - F_c = 2b_f(x - h_t) \cdot \frac{f_y}{\gamma_a} \quad \Rightarrow \quad x_a = \frac{(N_{a,pl} - F_c) \cdot \gamma_a}{2 f_y b_f} + h_t, \tag{13}$$

and the resisting moment is

$$M_{Rd} = N_{a,pl} \cdot (h_g + h_t - \frac{x_c}{2}) - (N_{a,pl} - F_c) \frac{x_a - x_c + h_t}{2}. \tag{14}$$

If the second neutral axis lies within the steel web, the stress blocks are as shown in Fig. 10c, and its value is determined through horizontal equilibrium

$$N_{a,pl} - F_c = 2b_f t_f \cdot \frac{f_y}{\gamma_a} + 2t_w(x_a - h_t - t_f) \cdot \frac{f_y}{\gamma_a}, \tag{15}$$

$$x_a = \frac{(N_{a,pl} - F_c) \cdot \gamma_a}{2 f_y t_w} - \frac{b_f t_f}{t_w} h_t + t_f. \tag{16}$$

Provided that

$$N_{aw} = N_{a,pl} - F_c - N_{acf} \qquad\qquad N_{acf} = 2b_f t_f \cdot \frac{f_y}{\gamma_a}, \tag{17}$$

the resisting moment is

$$M_{Rd} = N_{a,pl} \cdot (h_g + h_t) - F_c \frac{x_c}{2} - N_{acf}(h_t + \frac{t_f}{2}) - N_{aw} \frac{x_a + h_t + t_f}{2} .$$ (18)

In Fig. 11 is plotted the ratio $M_{Rd}/M_{pl,Rd}$ against the degree of shear connection $\eta = F_c/F_{cf}$ (curve ABC). When F_c is zero (no interaction) the resisting moment M_{Rd} is equal to the plastic moment of the steel member alone $M_{apl,Rd}$. Provided that the slip capacity of connectors is limited, the curve of Fig. 11 is not valid for very low degrees of shear connection (e.g. $F_c/F_{cf} < 0.4$).
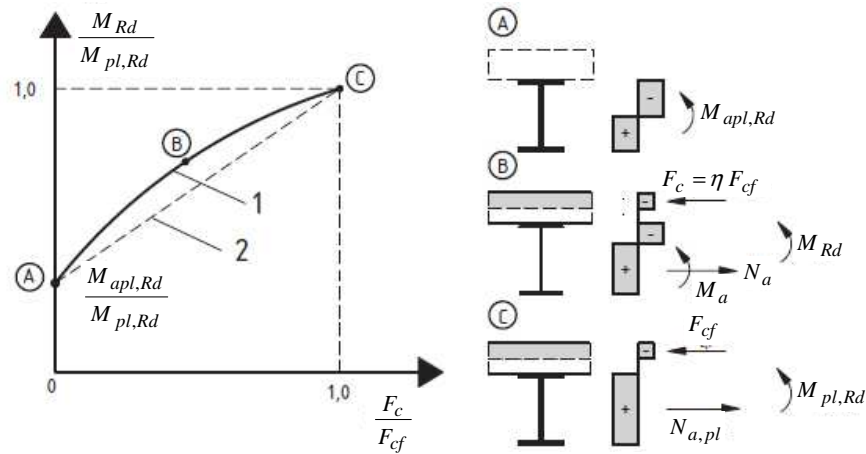
Figure 11 – Resisting moment against degree of shear connection.

Unfortunately, the curve ABC in Fig. 11 cannot be represented by a simple algebraic expression, so that in practice it is sometimes replaced by the line AC, given by

$$F_c = \left(\frac{M_{Sd} - M_{apl,Rd}}{M_{pl,Rd} - M_{apl,Rd}} \right) \cdot F_{cf} .$$ (19)

In design, M_{Sd} is known, $M_{pl,Rd}$, $M_{apl,Rd}$ and F_{cf} may be easily calculated, so Eq. (19) gives directly the design force F_c that has to be resisted with shear connectors. The number of connectors needed may be obtained from the relation

$$N = N_f \cdot \frac{F_c}{F_{cf}} = \frac{F_c}{P_{Rd}} ,$$ (20)

where P_{Rd} is the design resistance of one connector.

4.1.2   Resistance to hogging bending moment

As stated above the tensile resistance of the concrete is neglected. In the most common cases the neutral axis lies within the web of the steel member. The steel bottom flange is in compression, and its class is easily found, as stated in section 3.2. To classify the web, the position of the plastic neutral axis must be found. The design in hogging moment regions is based on the use of full shear connection.

Let A_r be the effective area of longitudinal reinforcement within the effective width b_{eff} of the slab. The tensile force in this reinforcement is

$$F_s = \frac{A_r f_{sk}}{\gamma_s},$$ (21)

where f_{sk} is its characteristic yield strength.

Without any tensile reinforcement in the slab, the bending moment is that of the steel element

$$M_{apl,Rd} = \frac{f_y W_a}{\gamma_a} = F_a \cdot z_a,$$ (22)

where W_a is the plastic section modulus, f_y is the yield strength, F_a is the resultant force of the stress blocks in compression and tension in case of the steel member alone, z_a is the lever arm. For rolled sections the values of W_a are tabulated, whereas for plate girders F_a and z_a have to be calculated. To consider the contribution of the slab reinforcement it may be assumed that the stress in a depth x_c of the web changes from tension to compression, where x_c is given by

$$x_c t_w \frac{2f_y}{\gamma_a} = F_s.$$ (23)

Provided that (as is usual)

$$x_c \leq \frac{h_a}{2} - t_f.$$ (24)

The depth of web in compression is then

$$\alpha c = \frac{d}{2} + x_c,$$ (25)

using Table 1 it is possible to define the class of the web. If the class is 3 or 4, the elastic analysis has to be used.

The lever arm for the two forces F_s (Fig. 12b) is given by

$$z = \frac{h_a}{2} + h_s - \frac{x_c}{2},$$ (26)

where h_s is the height of the reinforcement above the interface. The moment of resistance is

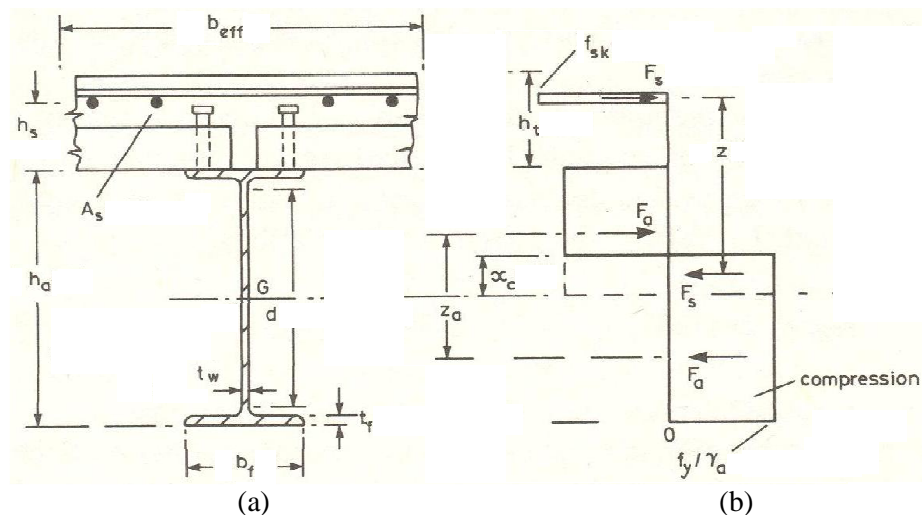$$M_{h,Rd} = M_{apl,Rd} + F_s z.$$ (27)

Figure 12 – Resistance to hogging bending of composite section (full shear connection).

This procedure is also possible to be used also for sections with flanges in class 1 or 2 and web in class 3, by neglecting a region in the center of the compressed part of the web, to account for local buckling (hole-in-the-web method).

5 Elastic analysis of composite sections to bending moment

As stated in section 4, the resistance of sections in class 3 and 4 has to be calculated with reference to elastic analysis. Moreover the evaluation of stresses in service for all section classes has to be done according to elastic analysis.

It is assumed first that full shear connection is provided, so that the effect of slip can be neglected. All other assumptions are as for the elastic analysis of reinforced concrete sections by the method of transformed sections. The algebra is different because the flexural rigidity of the steel section alone is much greater than that of reinforcing bars. The modular ratio for short term loading is $n=E_a/E_c$, with suffixes a as steel and c as concrete.

5.1 Sections in sagging bending

For generality, the considered steel section is assumed to be asymmetrical (Fig. 13) with cross sectional area A_a, second moment of area I_a, and center of area distance below the top surface of the concrete slab z_g, which has overall thickness h_t and effective width b_{eff}. It is usually neglected the reinforcement in compression, the concrete in tension and the concrete between the ribs of profiled sheeting, even when the sheeting ribs are parallel to the steel member. The neutral axis lies in the slab if the following inequality is satisfied

$$A_a\,(z_g - h_c) < \frac{1}{2} b_{eff} \frac{h_c^2}{n}\,. \tag{28}$$

The neutral axis depth is obtained by equating the first moments of area

$$A_a\,(z_g - x) = \frac{1}{2} b_{eff} \frac{x^2}{n}\,, \tag{29}$$

and the second moment of area, in steel units, by

$$I = I_a + A_a\,(z_g - x)^2 + b_{eff} \frac{x^2}{3n}\,. \tag{30}$$

If the inequality (28) is not satisfied, the neutral axis depth is greater than h_c

$$A_a\,(z_g - x) = b_{eff}\,h_c \frac{x - h_c/2}{n}\,. \tag{31}$$

The second moment of area is

$$I = I_a + A_a\,(z_g - x)^2 + \frac{b_{eff}\,h_c}{n}\left[\frac{h_c^2}{12} + \left(x - \frac{h_c}{2}\right)^2\right]\,. \tag{32}$$

The stresses due to a sagging bending moment M are calculated at the top of the concrete slab (level 1 in Fig. 13) and at top and bottom of the steel member (levels 3 and 4, respectively). The stresses, with tensile stress positive, are

$$\sigma_{c1} = -\frac{M\,x}{n\,I}\,, \tag{33}$$

$$\sigma_{a3} = \frac{M\,(h_t - x)}{I}\,, \tag{34}$$

$$\sigma_{a4} = \frac{M\,(h_a + h_t - x)}{I}\,. \tag{35}$$

In case of unpropped construction at the stresses calculated on the composite section, the stresses acting on the steel member alone, due to own weight of the composite beam, have to be added.
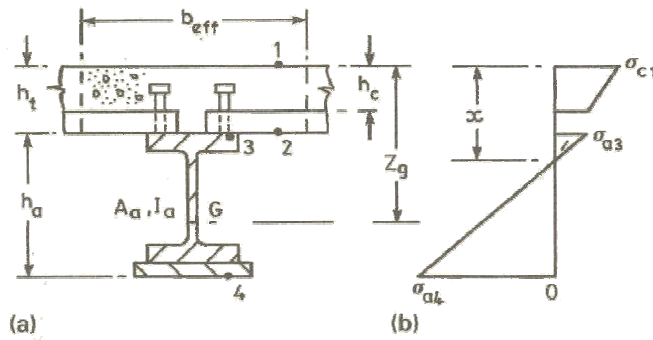
Figure 13 – Elastic analysis of composite section in sagging moment.

5.2 Sections in hogging bending

Similarly to sections in sagging bending, the height x of the elastic neutral axis of the composite section is obtained from the first moment of area

$$A_a\,(z_g - x) = A_s\,(x + h_s - h_t), \tag{36}$$

where h_s is the distance of the reinforcement from the top of the steel profile, as in Fig. 12. The second moment of area of the composite section is

$$I = I_a + A_a\,(z_g - x)^2 + A_s\,(x + h_s - h_t)^2. \tag{37}$$

So the stresses at the extreme fibers of the steel element are calculated using the Eqs. (34) and (35); the stresses in the reinforcement are calculated with the relation

$$\sigma_{s1} = \frac{M\,(h_t - h_s - x)}{I}\,. \tag{38}$$

In case of unpropped construction, the stresses in the steel member due to the own weight of the steel joist and the concrete slab have to be added to those acting on the composite beam.

5.3   Effects of shrinkage of concrete

The concrete in a fairly dry environment is expected to shrink. In a composite beam, the shrinkage of the slab is restrained by the steel member, causing a tensile force in the concrete through shear connectors near the free ends of the beam. The forces on the shear connectors act in the opposite direction to those due to the loads, and so can be neglected in the design.

For the evaluation of section stresses due to shrinkage on consider a portion of the composite beam of unitary length (Fig. 14). (a) Firstly the portion of beam is assumed fictitiously fixed at the extremities. Due to the restrained shrinkage of concrete slab, a tensile force occurs in the support in correspondence of the centroid of the slab

$$N_{sh} = E_{cm} A_c \, \varepsilon_{sh} = \frac{E_a}{n} A_c \, \varepsilon_{sh} \,, \tag{39}$$

where ε_{sh} is the longitudinal strain due to shrinkage. The concrete slab is subjected to a uniform tensile stress

$$\sigma_c(a) = E_{cm} \, \varepsilon_{sh} \,. \tag{40}$$

(b) On remove the fictitious restraints and on apply the axial force N_{sh}, with opposite sign, on the centroid of the concrete slab. The composite element is then subjected to a combined compression and bending and so the stress value at the generic fiber of the concrete slab distant x from the top of the section is

$$\sigma_c(b) = -\frac{N_{sh}}{nA} - \frac{M_{sh}}{nI} \, (z_c - x) \,, \tag{41}$$

where A, I are the area and the second moment of area of the homogenized composite section with the elastic modulus ratio n; z_c is the position of the centroid of the composite section with respect to the top of the section, and

$$M_{sh} = N_{sh} \, (z_c - h_c/2) \,. \tag{42}$$

The effective stresses are then obtained as the superposition of the stresses obtained in phase (a) and those obtained in phase (b) (Fig. 14)

$$\sigma_{c,t}(a+b) = \frac{N_{sh}}{A_c} - \frac{N_{sh}}{nA} - \frac{M_{sh}}{nI} \, z_c \tag{43}$$

$$\sigma_{c,b}(a+b) = \frac{N_{sh}}{A_c} - \frac{N_{sh}}{nA} - \frac{M_{sh}}{nI} \, (z_c - h_c) \tag{44}$$

$$\sigma_{s,t}(a+b) = -\frac{N_{sh}}{nA} - \frac{M_{sh}}{nI} \, (z_c - h_t) \tag{45}$$

$$\sigma_{s,b}(a+b) = -\frac{N_{sh}}{nA} + \frac{M_{sh}}{nI} \, (h_a + h_t - z_c) \,. \tag{46}$$

Actually, the stresses due to shrinkage develop slowly, and so they are reduced by creep of the concrete. For simplicity, a reduced modulus of elasticity for the concrete $E_{c,eff}$ may be considered to account for the attenuation effect provided by creep (see section 5.4); then in the Eqs. (43-46) a greater modular ratio has to be used ($n_{eff} = [1 + \chi(t,t_0) \, \varphi(t,t_0)] \, n$). The value of $\chi(t,t_0)$ in this case can be assumed equal to 0.5 (Eurocode 4-2004) because the stresses at t_0 are zero and as they increase the creep coefficient decreases.
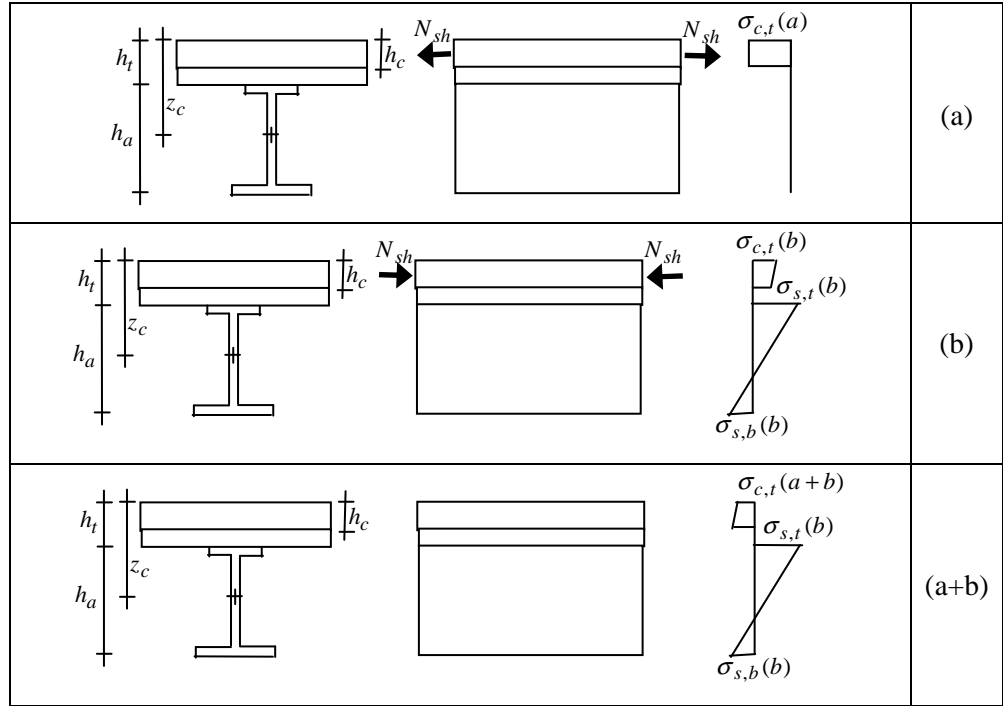
Figure 14 – Shrinkage effect: (a) tensile stresses in the slab due to restrained shrinkage, (b) stresses in the composite beam due to the eccentric compression N_{sh}, (a+b) sum of the effects.

5.4 Effects of creep of concrete

As well known, the deformation of concrete elements subjected to permanent loads increases with time due to creep. So connecting concrete with steel, as in composite structures, considerable stress redistributions between the two materials occur along the time (Eurocode 2-2004, CEB-FIP 1990). Generally this variation consists in a reduction of stress in the concrete slab and an increase in the steel element (Fig. 15).
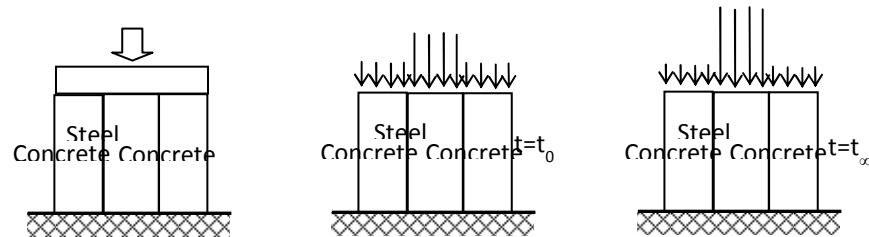
Figure 15 – Redistribution of stresses between steel and concrete due to creep.

Defining with $J(t,t_0)$ the creep function, that represents the deformation law with time due to a unitary stress applied at the instant t_0,

$$J(t,t_0) = \frac{1 + \varphi(t,t_0)}{E_c} , \qquad (47)$$

where $\varphi(t,t_0)$ is the creep coefficient, and represents the viscous part of the deformation. Provided that the stress varies with time, due to the redistribution between materials, and that the creep function is different per each starting time, the relation between deformation and stress at the generic instant t is as follow:

$$\varepsilon(t,t_0) = \sigma(t_0) J(t,t_0) + \int_{t_0}^{t} J(t,\tau) d\sigma(\tau) . \tag{48}$$

Both deformation and stress are unknown so that the problem requires solving a Volterra's integral equation (Eq. 48). In Fig. 16 it is represented graphically the Eq. (48); the area defined by the curve and the axis in the bottom right of the figure constitutes the deformation at the instant t of a phenomenon started at time t_0. The Eq. (48) may be solved by numerical integration (general method) or transforming through simplifications the superposition integral in an algebraic form. The most common method is AAEMM (Age Adjusted Effective Modulus Method), in which the stress variation $\sigma(t)$-$\sigma(t_0)$ is multiplied by an "average" value of the creep function $\mu(t,t_0)J(t,t_0)$ (Fig. 17), so Eq. (48) becomes

$$\varepsilon(t,t_0) = \sigma(t_0) J(t,t_0) + (\sigma(t) - \sigma(t_0)\mu(t,t_0) J(t,t_0) . \tag{49}$$

The function $\mu(t,t_0) \leq 1.0$ takes into consideration the variation of the stress with time and the reduction of the creep function due to ageing of concrete. A more useful function is $\chi(t,t_0)$ ≤ 1.0 that is applied on the creep coefficient so Eq. (49) becomes

$$\varepsilon(t,t_0) = \frac{\sigma(t_0)\,(1+\varphi(t,t_0))}{E_c} + \frac{(\sigma(t) - \sigma(t_0)(1+\chi(t,t_0)\varphi(t,t_0))}{E_c} . \tag{50}$$

Making some hypotesis on the variation of the stress with time it is possible to derive values of the coefficient $\chi(t,t_0)$; in most cases may be assumed equal to 0.8. Another algebraic method, simpler than AAEMM, is the EMM (Effective Modulus Method) that assumes no ageing effect on the creep of concrete, so it assumes $\chi(t,t_0)$=1.0.
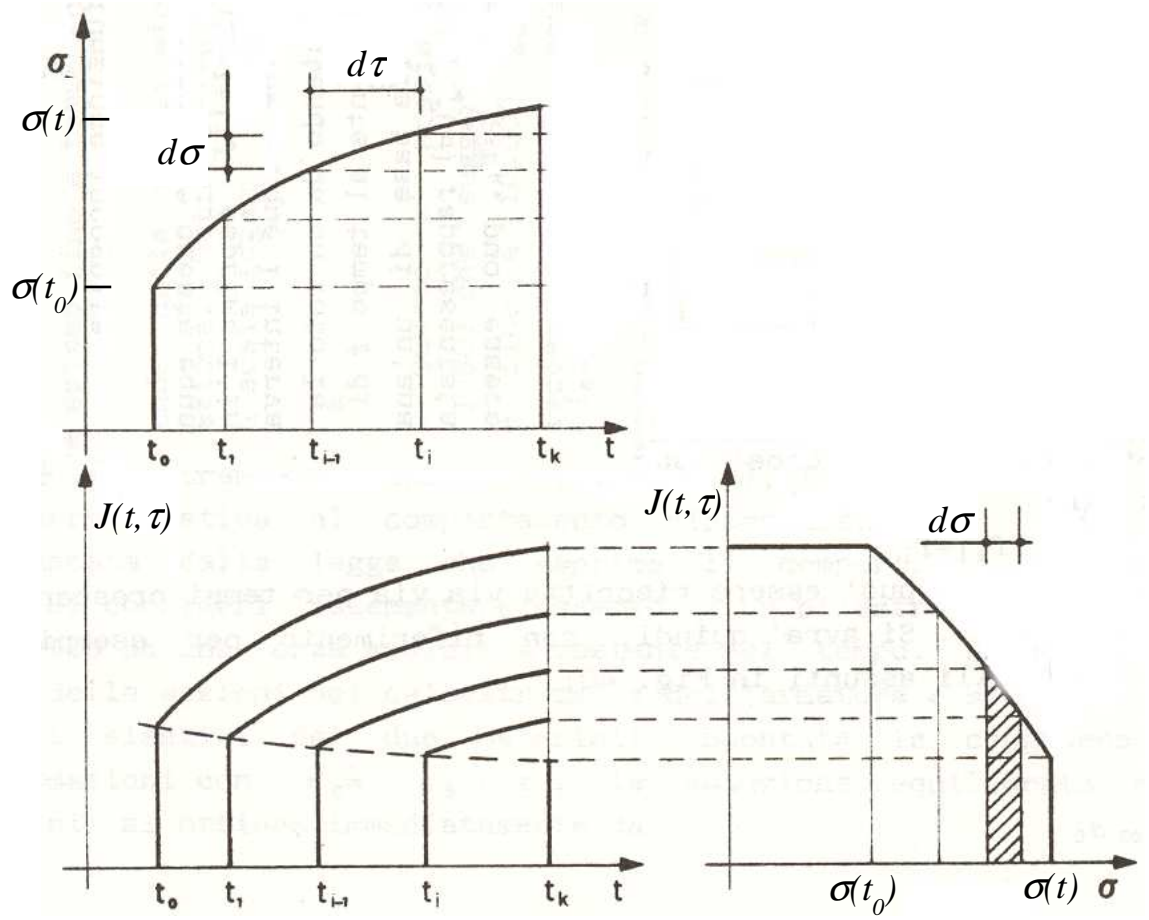
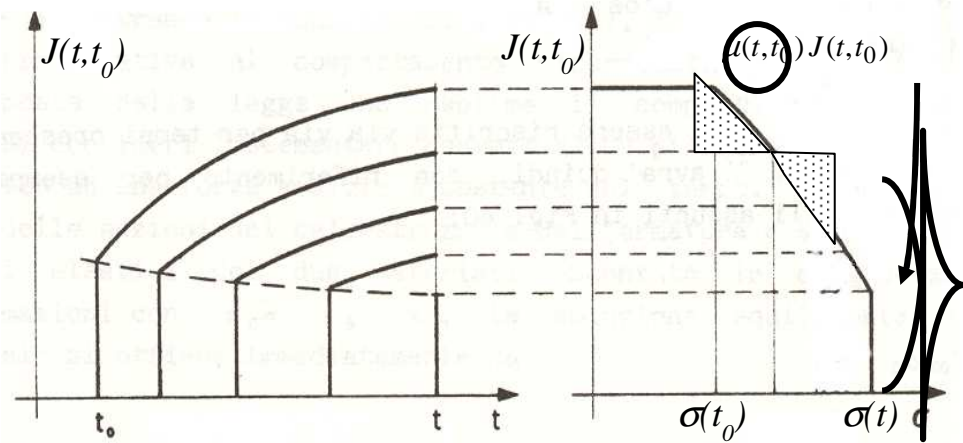Figure 16 – Graphical representation of Eq. (48).

Figure 17 – Graphical representation of Eq. (49).

In the simplest way, then, it is possible to consider the effects of creep using a reduced modulus of elasticity (effective modulus) equal to

$$E_{c,eff}(t,t_0) = \frac{E_c}{1+\varphi(t,t_0)}. \tag{51}$$

So the Eq. (43-46) may be used to calculate the stresses due to permanent loads but considering a modular ratio

$$n_{eff} = \frac{E_a}{E_c}(1 + \varphi(t,t_0)) \, . \tag{52}$$

6 Serviceability limit states

In the design of structures, besides the checks concerning the bearing capacity, it is necessary to check if the requests in service are satisfied. These checks concern the values of the stresses in the materials, the deformation (flexural deflection) and the cracking of concrete. For the calculation of stresses in service the elastic analysis of the sections has to be used considering also the effects of creep and shrinkage (section 5). The values of the calculated stresses have to be not greater than some limits, which are normally: for concrete 0.45 f_{ck} under the quasi-permanent loading condition and 0.60 f_{ck} under the rare loading condition, for steel the yielding stress. Actually, in Eurocode 4 (2004) no limitations of stresses are requested for beams if, in ultimate limit state, no verification of fatigue is required and no pre-stressing by tendons and/or by controlled imposed deformations (e.g. jacking of supports) is provided.

6.1 Deflection

The correct evaluation of the deflection is of great importance especially in buildings because an excessive deflection may cause damage in fragile non structural elements and finishing parts. For continuous composite beams the cracking of concrete slab in hogging bending regions has to be considered.

Applying the principle of virtual works, it is possible to calculate the maximum deflection δ_c in one span of a continuous beam, in the hypothesis of full interaction, by the relation

$$\delta_c = \int_0^l M'(z) \cdot \vartheta(z)\,dz \, , \tag{53}$$

where $M'(z)$ is the moment due to a unitary force applied in the section of maximum deflection on a simply supported beam and $\vartheta(z)$ is the curvature evaluated on the real structure. The curvature may be assumed equal to $\vartheta_1(z)=M/E_aI_1$ for short term loading, to $\vartheta_{1,eff}(z)=M/E_aI_{1,eff}$ for long term loading and to $\vartheta_2(z)=M/E_aI_2$ for the zones subjected to hogging moment. I_1 is the second moment of area of the composite section in the uncracked condition of the slab, $I_{1,eff}$ is the same evaluated using the effective modulus for concrete to account for creep and I_2 is the second moment of area of the composite section without considering the cracked concrete. $\vartheta(z)$ may be evaluated considering the effect of tension stiffening through the relationship proposed by Favre for reinforced concrete structures

$$\vartheta(z) = \vartheta_1 \cdot \beta \left(\frac{M_{cr}}{M} \right)^2 + \vartheta_2 \cdot \left[1 - \beta \left(\frac{M_{cr}}{M} \right)^2 \right], \tag{54}$$

where β is a coefficient that considers the type of loading (1.0 for short term loads, 0.5 for long term loads or cyclic loads) and M_{cr} is the moment that causes the cracking of the slab. The cracking moment may be determined as

$$M_{cr} = n \cdot f_{ct} \cdot W_1, \tag{55}$$

where W_1 is the section modulus of the composite beam for negative bending moment with uncracked concrete and f_{ct} is the tensile resistance of concrete. In the latter case a numerical integration of the right term of Eq. (53) is needed.

For the evaluation of bending moments along the beam axis for the case of continuous composite beams a different stiffness has to be considered: $E_a I_1$ for sagging bending zones ($E_a I_{1,eff}$ for long term behavior) and $E_a I_2$ for hogging bending zones. The hogging zone may be assumed equal to 15% of the length of the adjacent spans.

Where the shear connection is partial ($N/N_f < 1$), the increase in deflection due to longitudinal slip depends also on the method of construction. The total deflection δ is given approximately (as suggested by Eurocode 4-2004) by the relation

$$\delta = \delta_c \cdot \left[1 + k \cdot \left(1 - \frac{N}{N_f} \right) \cdot \left(\frac{\delta_a}{\delta_c} - 1 \right) \right], \tag{56}$$

where δ_a is the deflection for the steel beam acting alone; the parameter k is equal to 0.5 for propped construction and equal to 0.3 for unpropped construction.

6.2 Cracking

Another important aspect concerning the behavior in service of a continuous composite beam is the cracking of the concrete slab in hogging bending regions. Cracking has to be limited to a level that does not impair the proper functioning of the structure, its durability or cause its appearance to be unacceptable. The problem is almost absent in simply supported beams because the concrete slab is mostly compressed with the exception of the external parts where the shrinkage causes some tensile stresses, which normally do not cause appreciable cracking.

The calculation of the crack width may be done integrating the difference between the steel strain ε_s and the concrete strain ε_c on the crack distance s_r

$$w_m = \int_0^{s_r} (\varepsilon_s - \varepsilon_c) \cdot dz. \tag{57}$$

The characteristic crack width w_k may be obtained simplifying Eq. (57) in an algebraic expression considering the average values of steel strain ε_{sm} and concrete strain ε_{cm} and the maximum distance between cracks $s_{r,max}$:

$$w_k = (\varepsilon_{sm} - \varepsilon_{cm}) \cdot s_{r,max}. \tag{58}$$

The difference of strains may be obtained (Eurocode 2-2004)

$$\varepsilon_{sm} - \varepsilon_{cm} = \frac{\sigma_s - k_t \cdot \dfrac{f_{ctm} A_{c,eff}}{A_r} \left(1 + n \dfrac{A_r}{A_{c,eff}}\right)}{E_s} , \tag{59}$$

where σ_s is the tensile stress in the reinforcement considering cracked the section, f_{ctm} is the average tensile resistance of concrete, A_r is the area of the reinforcement, $A_{c,eff}$ is the effective area of the concrete subjected to tension surrounding the reinforcement; for composite beams the slab is normally completely subjected to tension so that $A_{c,eff}=r\ 2.5 b_{eff}(c+\phi/2)$. The parameter r is the number of reinforcement rows, c is the concrete cover, ϕ is the bar diameter. The maximum crack spacing for slabs subjected to tension and reinforced with deformed bars is obtained from the relation (Eurocode 2-2004)

$$s_{r,\max} = 3.4c + 0.34 \frac{\phi A_{c,eff}}{A_s} . \tag{60}$$

The maximum allowable crack width varies from 0.1 mm to 0.4 mm in function of the environmental conditions and the loading combinations in service.

7 Global analysis of continuous beams

The subject of this section is the determination of design values of bending moment and vertical shear for continuous composite beams caused by the actions specified for both serviceability and ultimate limit states.

Elastic analysis may be applied for all limit states and for all classes of cross section. Rigid-plastic analysis, also known as plastic hinge analysis, is applicable only for ultimate limit states and for compact cross sections (class1). The latter is simpler because the design moments for one span are in practice independent of the actions on adjacent spans, the variation along the span of the stiffness of the member, the sequence and method of construction, and the effects of temperature and of creep and shrinkage of concrete. Nonlinear analysis may also be applied for both ultimate and serviceability limit states, but this analysis has to be carried out through sophisticated numerical procedures (e.g. Kristek & Studnicka 1982, Aribert & Aziz 1986, Salari et al 1998, Gattesco 1999).

7.1 Elastic analysis

To carry out elastic global analysis it is necessary to know the values of flexural stiffness *EI* over the all length of the structure. Per each cross section different values of *EI* are required:

a) for the steel member alone $E_a I_a$, for actions applied before the member becomes composite, where unpropped construction is used;

b) for permanent loading on the composite member $E_a I'_1$, for uncracked sections (sagging bending regions), where I'_1 is determined, in 'steel units', by the application of transformed sections using a modular ratio $E_a/E_{c,eff}$ to account for creep of concrete;

c) for variable loading on the composite member E_aI_1, for uncracked sections (sagging bending regions), where I_1 is determined, as above, but using a modular ratio E_a/E_c;

d) for all loading on the composite member E_aI_2, for cracked sections (hogging bending regions), where I_2 is determined neglecting the concrete in tension (cracked) but including the reinforcement.

To account for the effects of cracking of concrete in hogging moment regions it is necessary to consider in the analysis a different stiffness in cracked and uncracked sections. It is not easy to know 'a priori' which parts of each span are cracked; however a common assumption is that 15% of each span (Fig. 18), adjacent to each internal support, is cracked (e.g. Eurocode 4-2004).
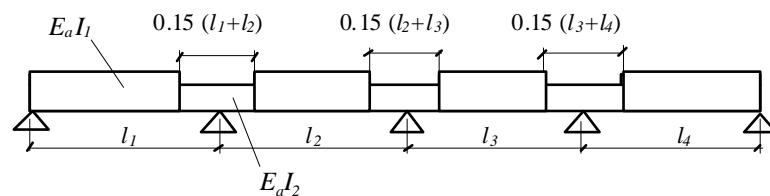
Figure 18– Flexural stiffnesses along the beam.

At ultimate limit state, to account also for the inelastic behavior of materials before the maximum load is reached, a limited moment redistribution may be applied. In practice also uncracked analysis is frequently used to calculate the moments at ultimate limit states, and modifying the results 'a posteriori' to consider both the inelastic behavior that occurs in all materials and the effects of cracking. In most codes of practice (e.g. Eurocode 4-2004) the maximum values of moment redistribution that guarantee the respect of rotation compatibility in correspondence of the continuity supports are reported. These limits are referred both to cracked and uncracked elastic analysis (Table 3). For serviceability limit states (stresses, deflection, crack width) only the cracked elastic analysis has to be used.

The moment redistribution limits reported in Table 3 may vary considerably in case of using steel for the reinforcement with low ultimate uniform strain. Moreover the moment redistribution limits have to be related also to the serviceability limit states so to guarantee that the redistribution applied do not causes an excessive crack or deflection in the composite beam. A specific study on this concern may be found in (Gattesco et al. 2010) and a summary is presented and discussed in section 8.

Table 3 – Maximum percentage of redistribution of elastic hogging moments.

Class of cross section in hogging moment region	1	2	3	4
For uncracked analysis	40	30	20	10
For cracked analysis	25	15	10	0

7.2 Rigid-plastic analysis

Rigid-plastic analysis of continuous composite beams may imply even large redistributions of elastic moments as a consequence of inelastic rotations in correspondence of internal supports. Rotations may be limited either by crushing of concrete or buckling of steel, and so depends on the proportions of the relevant cross sections, as well as on the shape of the constitutive relationships of the materials. So that some limitations to the use of rigid-plastic global analysis have to be fixed as (e.g. Eurocode 4-2004):

a) at each plastic hinge location: lateral restraint has to be provided, the effective section has to be in class 1, the steel component of the cross section has to be symmetrical about the plane of its web;
b) all effective cross sections in the member have to be in class 1 or 2;
c) adjacent spans have not to differ in length by more than 50% of the shorter span;
d) end spans have not to exceed 115% of the length of the adjacent span;
e) the member has not to be susceptible to lateral-torsional buckling.

The method of analysis is well known, being widely used for steel-framed structures, so only an outline is given here. The main assumptions are the following

1) the collapse of the structure occurs by rotation of plastic hinges at constant bending moment, all other deformations being neglected;
2) where the bending moment due to actions reaches the bending resistance of the member forms a plastic hinge;
3) the loads increase in proportion until failure occurs, so the load may be represented by a single parameter (load multiplier λ_p).

(a)   (b)
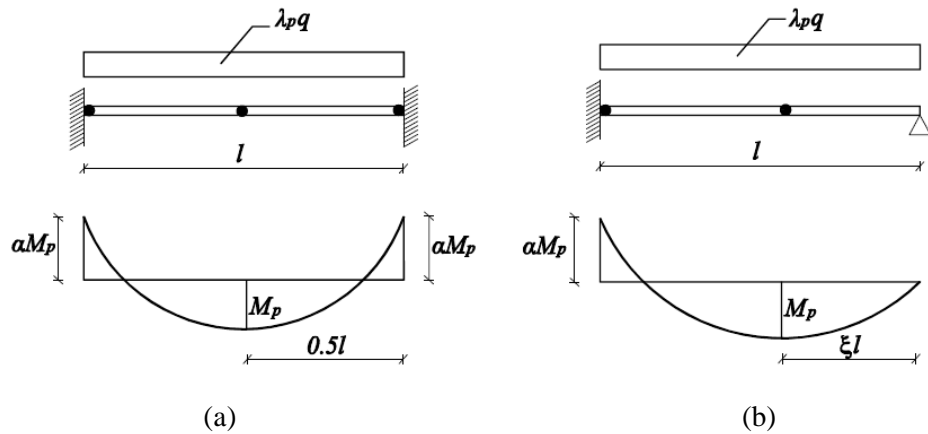
Figure 19 – Rigid-plastic global analysis: (a) fixed ended beam and (b) propped cantilever.

For an assigned collapse mechanism, by equating the potential energy of the loads, due to a small movement of the mechanism, with the energy dissipated in the plastic hinges on obtain the value of the load multiplier associated to the beam capacity (Gattesco et al. 2010). In particular for the beam with fixed ends (Fig. 19a) and for the propped cantilever (Fig. 19b) on obtain

$$
\begin{cases}
\xi\alpha M_p + M_p = \dfrac{\lambda_p q l^2}{2}\xi(1-\xi) & (for\ propped\ cantilevers) \\[2mm]
\alpha M_p + M_p = \dfrac{\lambda_p q l^2}{8} & (for\ fixed-end\ beams)
\end{cases} , \qquad (61)
$$

where ξ signifies the distance of the cross-section of maximum sagging bending moment from the pinned support, M_p is the moment of resistance at midspan, α is the ratio between the moment of resistance at support and that at midspan, q is the load. By solving Eqs. (61), the load multipliers λ_p may be obtained

$$
\begin{cases}
\lambda_p = \dfrac{4M_{p2}}{q l^2}\left(1 + \dfrac{\alpha}{2} + \sqrt{1+\alpha}\right) & (for\ propped\ cantilevers) \\[2mm]
\lambda_p = \dfrac{8M_{p2}}{q l^2}(1+\alpha) & (for\ fixed-end\ beams)
\end{cases} \qquad (62)
$$

8 Redistribution of moments

In continuous steel-concrete composite beams used for building floors, steel beams and joists are usually characterized by uniform cross-section along the entire length. In the regions of hogging bending moment, the full strength capacity of the composite section can never be achieved. The concrete slab, being in tension, normally cracks before the yielding of reinforcing bars, whereas the steel profile, being in compression, may suffer from local buckling phenomena. The moment capacity of the composite cross-section is therefore lower at the interior supports than in the regions of sagging bending moment. Conversely, the bending moment diagram calculated as a result of an elastic analysis is usually higher at the interior supports than at midspan. To fully exploit the moment capacity of the beam along the whole length, a significant redistribution of bending moment from interior supports to midspan is therefore needed. Such redistribution can only take place if sufficient plastic rotation capacity is available at the support so as to satisfy the rotation compatibility condition.

Several experimental studies were carried out in the past on the evaluation of plastic rotation capacity of steel sections (Lukey & Adams 1969, Kemp 1986). Those studies proved that the main parameters affecting the plastic rotation capacity are: (i) the lateral slenderness ratio of the flange in hogging moment region; and (ii) the width-to-thickness ratio of the compression flange and web. Further studies (Kemp & Dekker 1991) lead to the definition of some limits for the width-to-thickness ratio of steel flanges to prevent local buckling in composite beams. These limits were found on the basis of a critical compressive strain which was derived from theoretical and experimental studies in literature (Kemp 1985). Afterwards such a critical strain was employed to identify the onset of local buckling in continuous composite beams subjected to hogging bending moment (Kemp & Nethercot 2001).

Further research (Fabbrocino et al. 1998, Gattesco & Gasparotto 2003) on the plastic rotation capacity of compact composite sections (i.e. class 1) pointed out that a number of other parameters such as the shape of the steel cross-section, the ductility of reinforcing steel, the type of restraints, the load distribution and the degree of shear connection should be investigated since they can significantly affect the plastic rotation capacity. Research carried

out on reinforced concrete structures (Cosenza et al. 1993, Bigaj-van Vliet & Mayer 1998, Beeby 1998) pointed out that a significant reduction in plastic rotation capacity takes place when reinforcing steel with low ductility is used. In such cases, therefore, a reduced allowable percentage of moment redistribution can be expected.

Besides the compatibility request at ultimate limit state (ULS), also the serviceability requirements (e.g. cracking, deflection) have to be satisfied so as to ensure acceptable performance at serviceability limit state (SLS). Moment redistribution from the interior support to the midspan causes cracking of the concrete slab near the support, therefore the crack width in the concrete slab should be kept below an acceptable value when evaluating the allowable redistribution domain. Creep and shrinkage of concrete will increase the deflection and the crack width in the long-term under the quasi-permanent load condition, and therefore need to be considered for the evaluation of the permissible moment redistribution.

The outcomes of a broad numerical investigation focused on the evaluation of the permissible redistribution limits in continuous steel-concrete composite beams with low ductility reinforcing steel ($\varepsilon_{ru} \geq 2.5\%$, class A according to CEB 1993) are detailed in (Gattesco et al. 2010). The local buckling phenomena were considered by limiting the steel strain in compression below the critical value suggested in (Kemp & Nethercot 2001). Both rotation compatibility (ULS) and maximum allowable crack width in the short- and long-term (SLS) were considered in the evaluation of the redistribution limit. An advanced finite element model (Gattesco 1999, Fragiacomo et al. 2004), purposely developed for nonlinear analyses of steel-concrete composite beams in the short- and long-term, was used. Propped cantilevers and fixed-end beams subjected to uniformly distributed load were analyzed, which represent two-span and multi-span symmetrical continuous beams, respectively. To generalize the results, the variation of the geometric parameters defining the cross section was considered, so as to include most of the cases of technical interest. Different types of beam, load and connection should also be considered.

8.1   Nonlinear numerical model

The numerical program is based on the use of a finite element with 10 degrees of freedom, which is made of two parallel Navier-Bernoulli's beams, representing the concrete slab and the steel profile, linked through a nonlinear spring, schematizing the connection (Fig. 20) (Gattesco 1999, Fragiacomo et al. 2004). Perfect bond is assumed between reinforcement and concrete slab. In the reality, some local slip will take place in the concrete after the formation of cracks, but the use of a modified stress-strain relationship for reinforcement, as suggested by the Model Code 90 (CEB 1993), which implicitly takes into consideration the tension stiffening effect, leads to an acceptable approximation.

The numerical procedure developed by Fragiacomo et al. (2004) can be used to perform short- and long-term nonlinear analyses. In short-term analyses, the behavior of all component materials is modeled through nonlinear constitutive relationships: the equation proposed by (Ollgard et al 1971) for the connection system, an elastoplastic stress-strain relationship with hardening for the steel profile, and the non-linear stress-strain relationship proposed in (Mander et al. 1988) for concrete in compression. The collapse occurs when the maximum compressive strain in the concrete, the maximum tensile strain in the steel

reinforcement, or the critical strain in compression in the steel profile due to local buckling (Kemp & Nethercot 2001) is attained.

In long-term analyses, the time-dependent phenomena of the concrete slab, creep and shrinkage, are taken into account (Fragiacomo et al. 2004). Concrete is regarded as linear-viscoelastic in compression by solving the Volterra's integral equation through a step-by-step procedure.
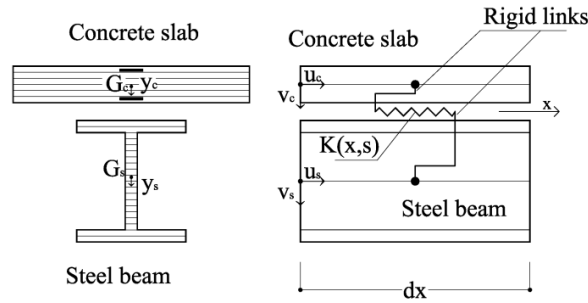
Figure 20 – Finite element model.

8.2 Evaluation of the allowable moment redistribution

The elastic analysis with limited moment redistribution allows the designer to consider the plastic behavior of the most stressed cross-sections without carrying out onerous nonlinear analyses. Simple closed form solutions can be implemented in an user-friendly spreadsheet which allows the designer to better exploit the strength and deformation capacity of all component materials leading to an optimized design of steel-concrete composite beams. The maximum elastic bending moments, generally at the interior supports, are reduced and the sagging bending moments at midspan are increased so as to satisfy the equilibrium with external loads (Fig. 21). The allowable moment redistribution percentage is limited, however, by the compatibility of the rotations in the critical cross-sections at ULS, and by the maximum crack width in the concrete slab in the short- and long-term at SLS.
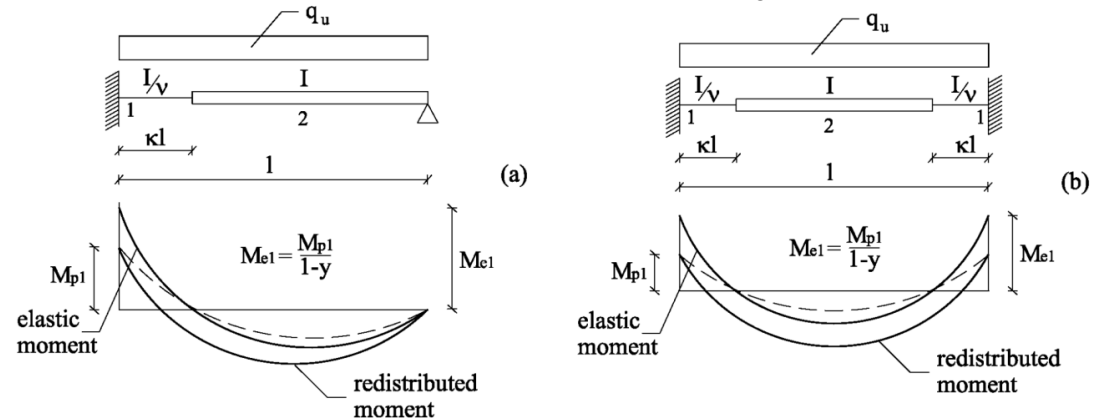
Figure 21 – Redistribution of elastic moments: (a) propped cantilever, (b) fixed-end beam.

8.2.1 Ultimate limit state

The permissible moment redistribution for a continuous beam at ULS can be calculated as a function of the maximum load that the beam can support (Gattesco & Cohn 1989). Such a

load depends on the type of collapse mechanism experienced by the structure. The collapse may occur when the rotation in the most stressed cross-section due to a load q_{u1} is equal to its actual rotation capacity (collapse due to "ultimate rotation"). Alternatively, the collapse may occur when the load q_{u2} leads to the formation of a number of plastic hinges that make the structure unstable (section 7.2). The actual collapse load will be the lesser of these two values. In the former case, the ultimate load q_{u1} can be determined by carrying out a nonlinear analysis to failure. The procedure is explained in detail for two different beams subjected to uniformly distributed loads: a propped cantilever, which represents half the symmetric two-span continuous beams, and a fixed-end beam, which represent the inner span of a multi-span continuous beam.

In the first step, the geometrical and mechanical properties of the composite beam (steel profile, concrete slab, slab reinforcement and shear connection) are defined in both sagging and hogging bending moment regions. A numerical analysis of the beam is then carried out up to the attainment of the collapse condition (either ultimate uniform elongation of steel bars in hogging moment section or critical strain in compression flange for local buckling) using the numerical program described in Section 8.1 so as to evaluate the ultimate load capacity q_{u1}. The expression proposed in Kemp & Nethercot (2001) for the critical compressive strain ε_{fb} in the flange of steel profile to account for local buckling was used:

$$\varepsilon_{fb} = 1.33 \cdot \left(\frac{t_f}{b_f}\right)^2 + 6.6 \cdot \left(\frac{t_f}{L_p}\right)^2 , \tag{63}$$

where t_f and b_f are the thickness and the breadth of the compression flange, L_p is the yielding length of the flange, which was assumed equal to 1.7 times the depth of the steel member (Kemp & Nethercot 2001).

The elastic hogging bending moment at the support can be calculated using the equation:

$$M_{e1} = -\frac{q_{u1} l^2}{\lambda} \mu , \tag{64}$$

where λ is a coefficient dependent upon the type of restraints at the ends of the beam and μ is a coefficient dependent to the type of beam. The ratio between the flexural stiffness of the cross-section under sagging and hogging bending moment is indicated with v and the ratio between the length of the beam subjected to hogging bending moment and the length l of the entire beam with κ (Fig. 21); then, for the propped cantilever beam, λ=8, κ=0.25, μ is obtained from the equation:

$$\mu = \frac{1 + \kappa^2 (v-1)(6 - 8\kappa + 3\kappa^2)}{1 + \kappa(v-1)(3 - 3\kappa + \kappa^2)} , \tag{65}$$

and, for fixed-end beams λ=12, κ=0.20, μ is obtained from the equation:

$$\mu = \frac{1 + 2\kappa^2 (v-1)(3 + 2\kappa)}{1 + 2\kappa(v-1)} . \tag{66}$$

Eqs. (65), (66) were derived by solving the beams using the analytical methods of the theory of elasticity. The plastic moment M_{p1} in hogging moment regions is evaluated according to the Eurocode 4 (2004). The reduced hogging moment (M_{p1}) due to section

plasticization and moment redistribution is equal to the elastic moment M_{el} in the same section due to the ultimate load q_{u1} multiplied by the factor $(1-y_u)$, where y_u is the redistribution factor (Fig. 21). By expressing in Eq. (64) M_{el} as a function of M_{p1} and y_u, the equation becomes:

$$\frac{M_{p1}}{1-y_u} = \frac{q_{u1}l^2}{\lambda}\mu, \tag{67}$$

where the minus sign has been eliminated since the plastic moment is always assumed positive. The allowable moment redistribution percentage due to the attainment of the ultimate rotation capacity in the cross-section subjected to hogging bending moment can then be calculated with the equation:

$$y_u = 1 - \frac{M_{p1}}{q_{u1}l^2}\frac{\lambda}{\mu}. \tag{68}$$

Assigning $q_{u2}= \lambda_p q$, obtained with Eqs. (62), and substituting it in Eq. (68) and being α the ratio between plastic moments at support and midspan, the maximum moment redistribution factors for the collapse mechanism become:

$$\begin{cases} y_{u,\max} = 1 - \dfrac{2\alpha}{\left(1+\dfrac{\alpha}{2}+\sqrt{1+\alpha}\right)}\dfrac{1}{\mu} & (\textit{for propped cantilevers}) \\[4mm] y_{u,\max} = 1 - \dfrac{3\alpha}{2(1+\alpha)}\dfrac{1}{\mu} & (\textit{for fixed}-\textit{end beams}) \end{cases}, \tag{69}$$

The allowable moment redistribution factors $y_{u,all}$ have to comply with the condition $y_{u,all} \leq y_{u,max}$.

8.2.2 Serviceability limit state

By applying the redistribution factors to the results of an elastic analysis, as described in the previous Section, the compatibility of rotation and the limit equilibrium are satisfied. The structure, however, may still fail the serviceability limit state verifications (crack width, deflection) in the short- and long-term. Deflection can usually be controlled by adopting adequate span to depth ratios and, if necessary, by precambering the steel beam. The control of crack opening of concrete slab in hogging regions may be omitted if the redistribution of elastic moments does not exceed a value determined according to the following.

From the ultimate loads q_{u1} and q_{u2}, the service load may be derived considering the partial safety factors γ_g for permanent loads and γ_q for live loads, and for materials γ_m, since the ultimate loads (q_{u1}, q_{u2}) are evaluated using the design values of the material strength. Assuming, for the sake of simplicity, that the effect of the material safety factor is equal, throughout the beam length, to the ratio η between the characteristic plastic moment $M_{p1,k}$ and the design plastic moment $M_{p1,d}$ at the fixed end, and denoting with ζ the live to total load ratio, the relationship between the service and the ultimate load is:

$$q_{ser} = q_{ui} \frac{\eta}{\gamma_g (1-\zeta) + \frac{\gamma_q}{\psi} \zeta} \quad (q_{ui} = q_{u1} \ or \ q_{u2}),$$ (70)

For serviceability limit states in the short-term, the rare load condition must be considered, while the quasi-permanent load condition has to be considered in the long-term. The service load for short- and long-term, q_{ser1} and q_{ser2} respectively, will be calculated using Eq. (70) with the load combination factor $\psi=1$ for the rare and $\psi=\psi_2$ for the quasi-permanent load condition. The ζ ratio was assumed equal to 1/3 in the parametric analyses, while the other coefficients γ_g, γ_q and ψ_2 were assumed equal to 1.35, 1.5 and 0.3, respectively.

The acceptable crack opening w_k can be calculated as in Section 6.2 (Eq. 58). Then, the difference of strains (ε_{sm}-ε_{cm}) corresponding to an assigned permissible crack opening can be calculated from Eq. (58). The value of the service load q_{cr} which causes the attainment of this strain difference can be obtained from the nonlinear analysis. The corresponding ultimate load q_u can be evaluated by inverting Eq. (70) with $q_{ser}=q_{cr}$. The permissible moment redistribution y_{cr} can then be calculated by substituting the load q_u in Eq. (68).

The allowable moment redistribution to be used in the design of continuous steel-concrete composite beams is the lesser of the values obtained for ULS and SLS verifications. Such a value ensures that the beam designed at ultimate limit state using the moment redistribution approach will not fail the serviceability limit state of maximum crack opening of the concrete slab under the rare and quasi-permanent load conditions in the short- and long-term, respectively.

8.3 Parametric analysis

The domain of allowable moment redistribution was computed by analyzing a wide range of steel-concrete composite beams subjected to uniformly distributed load. The control of ultimate and serviceability limit states in the short- and long-term was carried out for both propped cantilever and fixed-end beams. The connection of beams was designed as a full shear connection. The mechanical properties of concrete, steel profile and reinforcing bars are reported in Table 4. Low ductility steel with the uniform elongation at maximum load $\varepsilon_{ru}=2.5\%$ and class 1 steel sections ($b_f/t_f<18$) were used in the analysis.

8.3.1 Choice of the geometrical properties of the beams
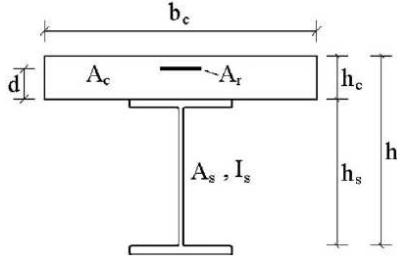
Some non-dimensional parameters were identified to represent the geometrical characteristics of steel-concrete composite beams (Johnson & May 1975). These parameters include the shape of the steel profile and concrete slab, the ratios between their cross-sectional areas and their depths, the ratio between the span length and the whole depth of the composite beam, and the ratio between the reinforcement and the profile steel areas at the hogging moment sections (Table 5).

Table 4 – Mechanical characteristics of steel, reinforcement and concrete.

Steel properties			Reinforcement properties			Concrete properties		
f_{sy}	275	MPa	f_{ry}	430	MPa	f_{ck}	30	MPa
ε_{sh}	1.5	%	f_{ru}	452	MPa	E_{cm}	33.600	MPa

ε_{su}	10.0	%	ε_{rh}	1.0	%	ε_{co}	0.20	%
E_s	210.000	MPa	ε_{ru}	2.5	%	ε_{cu}	0.35	%
E_{sh}	1.820	MPa	E_r	210.000	MPa			

Table 5 - Range of variation of the nondimensional geometrical parameters in the analysis.

Parameter		min. value	max. value	
Slab shape factor	b_e/h_e	5.80	28.0	
Concrete-steel depth ratio	d/h	0.11	0.40	
Steel profile shape factor	$I_s/A_s h_s^2$	0.15	0.19	
Steel-concrete area ratio	A_s/A_c	0.01	0.09	
Reinforcement-steel area ratio	A_r/A_s	0.04	0.50	
Span-depth ratio	L/h	20		

The choice of the beams was done so as to analyze steel-concrete composite beams with cross-sections representative of real structures. Most of the commercial rolled steel profiles such as taper flange beams (IPN), universal beams (IPE) and wide flange beams (HEB) with depths h_s=300, 600 and 900 mm and welded steel profiles with depths h_s=600 and 900 mm were considered. The concrete slab depth h_c was assumed equal to 150, 200 and 250 mm, while the concrete slab width was related to the span length in order to account for the shear-lag effect. Three values of the concrete slab width in the span were assumed: (i) the effective width, and (ii) two values obtained by multiplying the effective width by a reduction factor of 5/6 and 2/3, respectively, so as to include two cases with smaller spacing between adjacent steel profiles. The concrete slab width for the part of the beam over the support was taken as the lesser between the effective width at the support and in the span. The effective width was calculated in accordance with provisions of Eurocode 4 (2004). Three values of the ratio between the steel reinforcement A_r and the concrete slab area A_c were defined at the fixed supports, namely A_r/A_c=0.5%, 1.0%, 1.5%. The same cover of 30 mm from the upper fiber of the concrete slab was considered in all the analyses. An overall number of 224 beams, for both propped cantilever and fixed-end beams, were obtained by combining all the aforementioned geometrical parameters. The ranges of variation of non-dimensional parameters obtained for all possible combinations of steel profiles are summarized in Table 5; the combinations that do not correspond to possible cases were not considered in the analysis (Gattesco et al. 2010). The span length-depth ratio of the composite beams was assumed 20 in all analyses as this represents an average value commonly used in composite floor design.

8.3.2 Outcomes of the analyses

The numerical analyses carried out using the procedure previously described allowed the evaluation of the ultimate load capacity q_{ul} that leads to the attainment of the ultimate tensile strain in the reinforcing steel or the critical compressive strain in the steel profile for local buckling. With the same procedure, the service loads $q_{cr,1}$ and $q_{cr,2}$ corresponding to the attainment of a maximum crack opening in the concrete slab of 0.3 mm due to the rare and quasi-permanent load conditions, respectively, were also evaluated. While the load $q_{cr,1}$ was calculated through a short-term analysis, the load $q_{cr,2}$ was computed at the end of the service life by allowing for the time dependent phenomena (creep and shrinkage) of the concrete slab.

In all cases analyzed, the collapse load q_{u1} is associated to the attainment of either the elongation at maximum stress ε_{ru} of the reinforcing steel or the critical compressive strain ε_{fb} in the steel profile in the sections of hogging bending moment, where the maximum rotation capacity was reached. Even though the section of sagging bending moment inside the span was only partly plasticized in most of the cases analyzed, the ultimate load q_{u2} calculated using plastic analysis was frequently lower than the numerical load capacity q_{u1} (limited rotation capacity), mainly in the case of fixed-end beams

The permissible moment redistribution was evaluated with reference to uncracked composite sections, where the elastic internal forces were calculated by assuming the concrete as uncracked in tension.

In Figs. 22a,b the permissible moment redistribution determined considering ultimate limit state requirements (rotation compatibility and limit equilibrium) is plotted against the ratio A_r/A_s of the reinforcement to the steel profile area for propped cantilevers (Fig. 22a) and for fixed-end beams (Fig. 22b).
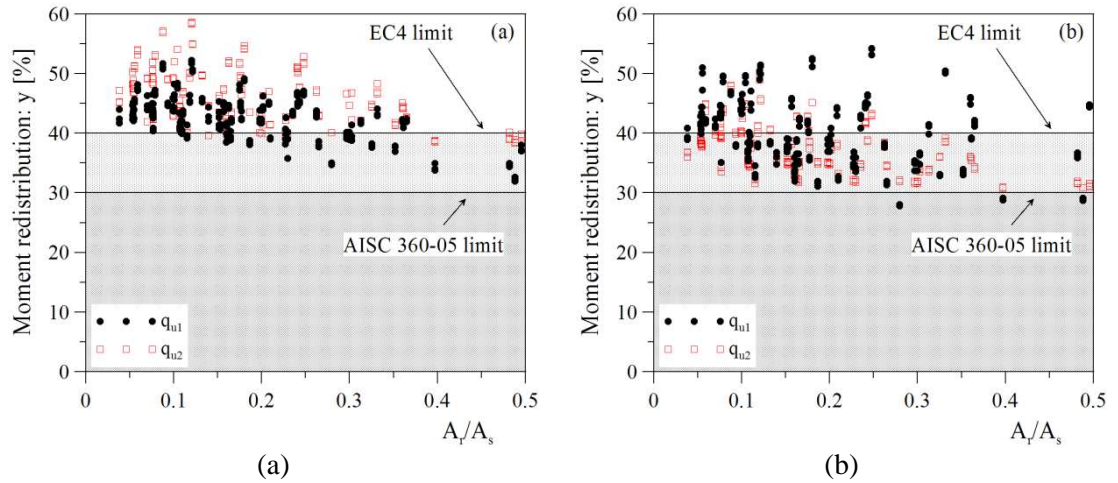

Figure 22 - Permissible moment redistribution at ULS versus the reinforcement ratio A_r/A_s for (a) propped cantilevers and (b) fixed-end beams for uncracked and cracked elastic analysis.

In the graphs, the limits of permissible moment redistribution suggested by the Eurocode 4 (2004) for class 1 composite sections and those suggested by AISC 360-05 (2005) are also evidenced. It can be noted that a significant number of the analyzed beams, particularly those with both fixed ends, showed values of the allowable redistribution ratio lower than that suggested by the Eurocode 4, but in any case larger than the redistribution limit suggested in AISC 360-05. The lower moment redistribution allowable in fixed ended beams is due to the higher plastic rotation demand in hogging sections with respect to propped cantilever (Gattesco & Cohn 1989). In summary, the results achieved show that the maximum redistribution value should be limited to 30%, as suggested by AISC 360-05, to avoid the collapse of critical sections due either to local buckling or to the rupture of the reinforcement.

In Figs. 23a,b and 24a,b, the permissible moment redistribution evaluated so as to comply with the serviceability requirement of control in the short-term of the maximum crack opening due to the rare load condition is plotted against the ratio A_r/A_s and A_r/A_c, respectively. A maximum crack opening of 0.3 mm, which is a reference value for most of the codes of practice for reinforced concrete slabs, was assumed. Figs. 23a, 24a refer to propped cantilevers, while Figs. 23b, 24b refer to fixed-end beams. The moment redistribution

percentages refer to internal forces calculated using an elastic analysis with uncracked section. In Figs. 23a,b and 24a,b both the permissible moment redistribution suggested by the Eurocode 4 (2004) and that suggested by AISC 360-05 (2005) are also reported. The results show that limited redistribution values are allowed for low values of the ratio A_r/A_s, but only for beams with a reinforcement percentage lower than 1.0% (Figs. 24a,b).

In order to draw a permissible moment redistribution domain, the moment redistribution value y=30%, that fulfils the ultimate limit state requirements, has to be reduced in the case of reinforcement ratio A_r/A_c less than 1.0 % to satisfy the serviceability limit state of 0.3 mm crack opening. In particular considering the two lowest limits of permissible moment redistribution for beams with 0.5% and 1.0% reinforcement ratio respectively (Figs. 24a,b), the following line can be obtained:

$$y = 80 \cdot \left(\frac{A_r}{A_c} - 0.005 \right). \tag{71}$$

Figure 23 - Permissible moment redistribution at SLS versus the A_r/A_s for (a) propped cantilevers and (b) fixed-end beams for uncracked elastic analysis.

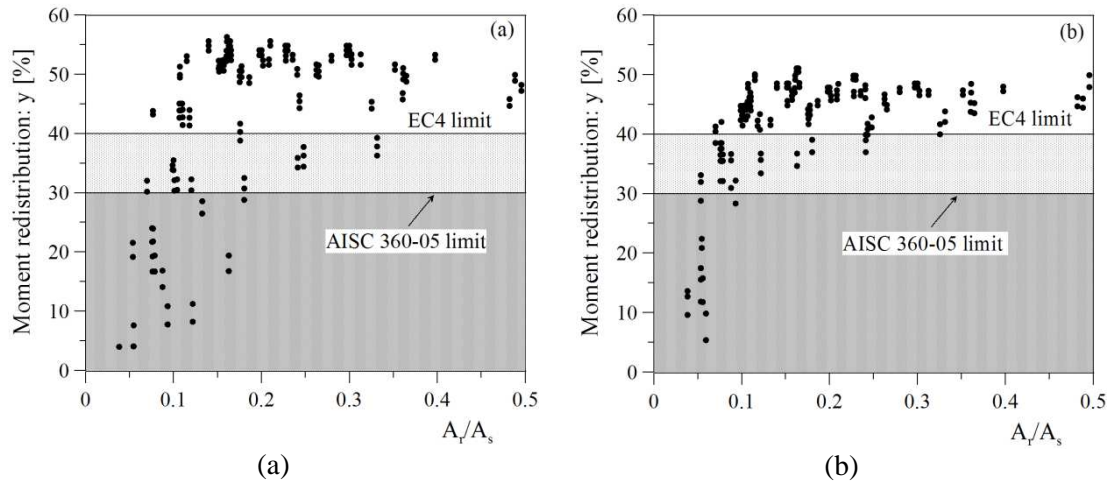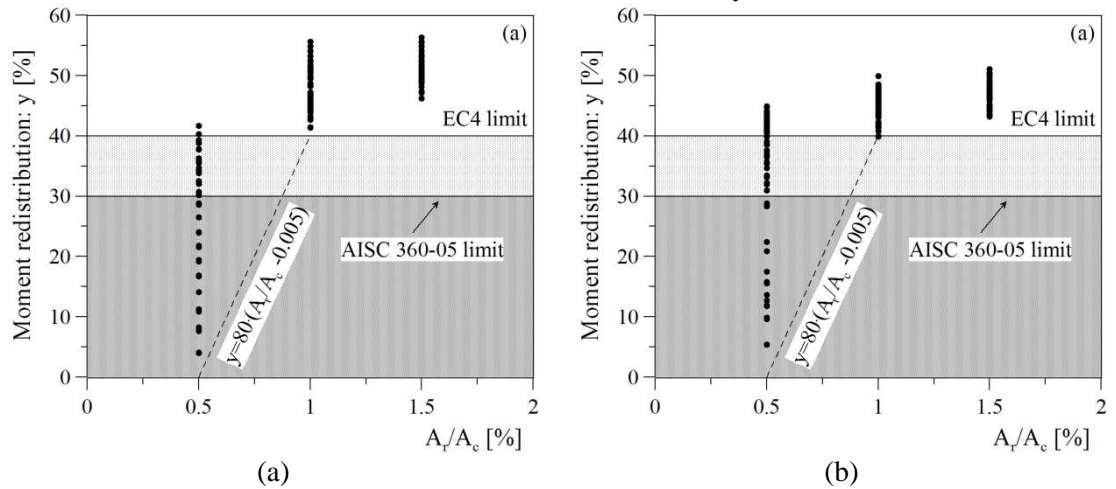Figure 24 - Permissible moment redistribution at SLS versus the A_r/A_c for (a) propped cantilevers and (b) fixed-end beams for uncracked elastic analysis.

9 Response of bridges to moving loads

Bridges are subjected to very complex loading conditions concerning mainly cyclic loads of different magnitude. Cyclic loads produce a progressive damage, more or less pronounced, in all parts of the structure. Actually the parts that are more sensitive to damage are bolted or welded joints and all parts where stress concentration occurs. Among these parts particular attention has to be paid to the connection between the concrete slab and the steel beam, because the presence of damage cannot be surveyed with any inspection method.

The loads acting on a bridge are moving commercial vehicles with different size and weight. For fatigue checks, most of codes of practice suggest to subdivide the variable cyclic stresses due to moving loads in a certain number of blocks of constant amplitude cyclic stresses according to an assumed cycle counting technique (e.g. rainflow, reservoir, etc.). Then the damage caused by a block of constant amplitude stresses is assumed proportional to the fraction of life used up by the event (ratio between the number of cycles and life to failure for the event); the total damage is obtained by summation of damage fractions due to each block of constant amplitude stresses (Miner's rule). In the procedure the damage varies linearly with the number of cycles and the connection behavior is considered linearly elastic.

Actually, the various types of vehicles crossing the bridge produce significantly different damage levels, which are not varying proportionally with the number of cycles and depend on the sequence of loading events. Particularly, the most heavy vehicles, even though they cross the bridge only few tenths of times per year, may cause the most part of the damage accumulated in the connection and moreover they can provoke the connection failure due to low-cycle fatigue (Gattesco et al. 1997).

These aspects are not yet a known cause of failures in service, probably because of some over-conservative points of the design, and because most composite bridges are still within the first third of their design life. However it is mandatory to develop numerical tools, able to simulate the actual behavior of composite bridge girders subjected to cyclic loads, which allow to preview the actual life to failure for new bridges and to assess the remaining life for existing bridges. It is, then, necessary to develop a numerical procedure able to study the structural behavior of composite beams subjected to moving loads and considering the actual cyclic relationship between the shear load and the slip of the connector.

A numerical tool able to simulate the behavior of bridge-type composite beams subjected to a particular non frequent fatigue loading model was presented in (Gattesco & Pitacco 2004). The procedure aims to determine the oscillogram of the slip, at steel-concrete interface, of each stud connector and to evaluate the damage caused by each slip cycle on the basis of slip-life fatigue curves.

9.1 Load-slip model for connectors

The constitutive relationships for concrete and steel are assumed linear elastic, whereas for the connection a nonlinear load-slip relationship is considered. In fact, the stresses in the steel member are normally below yielding and in the concrete slab are rather limited. On the contrary the load-slip curve of the connection is nonlinear even for very low values of the shear force and moreover the unloading curve is always different to the monotonic one (Gattesco 1997).
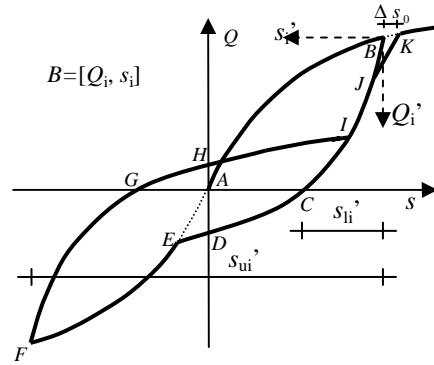
Figure 25 - Cyclic load-slip relationship of the connectors.

The cyclic load-slip relationship is derived from some experimental results (Gattesco & Rigo 1999) and it is illustrated in Fig. 25. The monotonic curve is described by the function

$$Q = \alpha \cdot \left(1 - e^{-\frac{\beta \cdot s}{\alpha}} \right) + \gamma \cdot s \tag{72}$$

where Q is the shear force, s is the slip between the concrete slab and the steel beam and the coefficients α, β, γ are constants experimentally determined (Tab. 6). The unloading curves refer to a local axis with the origin in points (Q_i, s_i) where the unloading starts (B in Fig. 25)

$$Q'_i = Q_i \cdot \lambda \cdot (1 - e^{-\frac{\eta \cdot z_i}{\lambda}} + \frac{\delta}{\lambda} \cdot z_i) \qquad \qquad with \ \ z_i = \frac{s'_i}{s'_{li}} \tag{73}$$

where s'_{li} is the slip, referred to the local axis, corresponding to a zero value of the load (point C) and it depends to the shear load ($s'_{li} = c_1 \cdot Q_i^3 + c_2 \cdot Q_i$), η has the expression $\eta = b_1 \cdot Q_i - b_2$ (≥ 0).

The coefficients λ (Eq. 73), c_1, c_2 and b_1, b_2 have to be experimentally determined (Table 6). The value of coefficient δ is obtained by Eq. (73) imposing $Q'_i = Q_i$ for $z_i = 1$ ($s'_i = s'_{li}$). The value of the slip at the end of the unloading s'_{li} varies with the number of cycles according to the relationship (Gattesco 1997, Gattesco & Giuriani 1996)

$$s'^{j}_{li} = s'^{1}_{li} \cdot \left(1 + \rho \cdot \frac{(j-1)^{\varepsilon}}{25 + (j-1)^{\varepsilon}} \right), \tag{74}$$

where ρ and ε are constants (Table 6) and j is the cycle number. At the first cycle the unloading curve ends at the intersection with the reverse monotonic curve (point E); a further increase of the negative load follows this curve (path E-F). From point F, the reloading curve has the same expression as Eq. (73) (path F-G-H-I) and it ends at the intersection with the first branch of the unloading curve of the preceding cycle (point I); an increase of the load follows this last curve up to point J and then the straight line J-K. A further increase beyond point K follows the monotonic curve. The new unloading curve follows a path similar to the reloading one with changed sign. If the unloading path (B-C-D) stops before point E, the reloading curve coincides with the unloading one up to point J.

The s'_{Ji} which defines point J is derived from the equation

$$-c_3 \cdot e^{-\frac{c_4 \cdot z_i}{c_3}} + c_5 \cdot z_i = 0 \qquad \left(c_3 = \frac{\Delta s_{oi}}{s'_{ui}} \right), \qquad (75)$$

c_4, c_5 are constants, s'_{ui} is the slip corresponding to the beginning of the reloading curve, referred to the local axis. The increment in slip Δs_{oi} at the end of the reloading curve (Fig. 25), which represents the damage at each cycle (crushing of concrete beneath the stud), may be determined in this way

$$\Delta s_{oi}^j = \frac{Q_i \cdot s'^j_{ui}}{s'^j_{li}} \cdot \left(\frac{\nu - \mu}{j} + \mu \right), \qquad (76)$$

where ν and μ are constants. The coefficients c_3 and c_4 vary with the number of cycles as follows

$$c_3^j = c_3^1 - \left(\frac{\Delta s_{oi}^1}{s'^1_{ui}} - \frac{\Delta s_{oi}^j}{s'^j_{ui}} \right), \qquad c_4^j = \frac{c_3^j}{c_3^1} \cdot c_4^1. \qquad (77)$$

Table 6 - Load-slip relationship coefficients for 19 mm stud connectors (f_y=350 MPa, f_t=450 MPa) embedded in concrete with compressive strength f_c=30 MPa (Gattesco 1997).

$\alpha = 82\ kN$	$\lambda = 0.90$	$c_4 = 2.3$	$\varepsilon = 0.85$
$\beta = 230\ kN/mm$	$b_1 = 0.054\ kN^{-1}$	$c_5 = 0.4$	$\rho = 0.31$
$\gamma = 5\ kN/mm$	$b_2 = 1.34$		
$c_1 = 9.2 \cdot 10^{-7}\ mm/kN^3$ $c_2 = 9.0 \cdot 10^{-4}\ mm/kN$		$\nu = 1.16 \cdot 10^{-4}\ mm/kN$ $\mu = 1.7 \cdot 10^{-5}\ mm/kN$	

9.2 Numerical model

The model of the composite beam consists of two one-dimensional elements, for steel beam and concrete slab, coupled by lumped springs, for shear connectors (Fig. 26). The main assumptions are: 1) linear behavior of the beams, both mechanically and geometrically; 2) the elements can slip along the connection without separation (i.e. uplifts neglected); 3) nonlinear behavior of lumped springs.
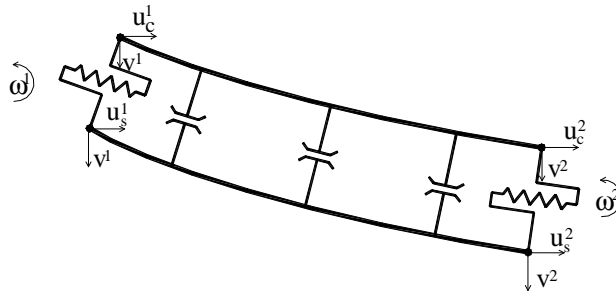

Figure 26 - Finite element considered in the numerical model.

The symbol $v(z)$ is used for the transverse displacement of the elements, $\omega(z)$ for section rotations, $u(z)$ for the axial displacements and $\gamma(z) = \omega(z) + v'(z)$ for the shear strain, where $v'(z)$ means the first derivative of v with respect to z. A subscript c or s is placed on the above symbols to refer them to concrete or steel element. The kinematics of the problem is described by the six fields $v_s(z)$, $\omega_s(z)$, $u_s(z)$, $v_c(z)$, $\omega_c(z)$, $u_c(z)$.

By assumption (2), the unknown fields are reduced to five by letting $v_s = v_c = v$ with the further consequence that $\omega_s - \omega_c = \gamma_s - \gamma_c$. As expected, and verified *a posteriori*, the shear strains γ are more than one order of magnitude smaller than rotations ω. Hence the approximation

$$\omega_s = \omega_c = \omega \;\Rightarrow\; \gamma_s = \gamma_c = \gamma \tag{78}$$

may be done, which allows to reduce the number of unknowns fields to four. By the above assumptions the shear slip of the i-th connector results

$$s_i = u_c(z_i) - u_s(z_i) + \omega(z_i)h, \tag{79}$$

where h is the distance between the centers of gravity of the two beams.

To develop a finite element formulation of the problem, it is temporarily assumed that the shear response Q_i is an external given quantity and that external forces are constant in time. Then the total mechanical energy is

$$J(v, \omega, u_s, u_c) = \frac{1}{2} \int_0^L \left[E_c A_c u_c'^2 + E_c A_c u_s'^2 \right] dz +$$
$$+ \frac{1}{2} \int_0^L \left[(E_c J_c + E_s J_s)\omega'^2 + (G_c A_c^* + G_s A_s^*)\gamma^2 \right] dz - \int_0^L p\,v\,dz - \sum_{i=1}^{N_c} Q_i s_i \tag{80}$$

where $p(z)$ is the transverse load, E_a and G_a the elastic constants, A_a, J_a the area and the second moment of the area of the sections and A_a^* the shear area. Introducing a finite element mesh of N_{el} beam elements with N_{no} nodes of coordinates z_j, $j = 1,...,N_{no}$, and four associated degrees of freedom

$$\mathrm{d}^j = \left[u_c(z_j), u_s(z_j), v(z_j), \omega(z_j) \right]^T \tag{81}$$

the energy functional could be written as

$$J = \frac{1}{2}\mathbf{KD} \cdot \mathbf{D} - \mathbf{F} \cdot \mathbf{D} + \mathbf{Q} \cdot \mathbf{D}, \tag{82}$$

where $\mathbf{D} \in \mathfrak{R}^N$ is the generalized displacement vector, N the total number of degrees of freedom, $\mathbf{K}$ is the stiffness matrix formed by assembling the concrete and steel beam elements, $\mathbf{F}$ is the external load vector, made by the contribution of the elements and node loads, and $\mathbf{Q}$ is the load vector formed by the connector contributions. While $\mathbf{K}$ and $\mathbf{F}$ are standard quantities to form, $\mathbf{Q}$ requires some further remarks. The connectors are placed at the nodes of the mesh so that the slip s_i of the connector placed at node x_i depends only on the degrees of freedom of that node by the relation $s_i = -\mathbf{b} \cdot \mathbf{d}^i$ where $\mathbf{b} = [-1,1,0,-h]$ (see Eq. 79). Called with $\boldsymbol{B}^i$ the vector of $\mathfrak{R}^N$ such that $\mathbf{B}^i \cdot \mathbf{D} = -\mathbf{b} \cdot \mathbf{d}^i$ for every $\mathbf{D} \in \mathfrak{R}^N$, ($\mathbf{B}^i$ is a vector with at most 3 components not zero) one gets

$$s_i = \mathbf{B}^i \cdot \mathbf{D}, \tag{83}$$

$$\mathbf{Q} = \sum_{i=1}^{N_n} Q_i \mathbf{B}^i, \tag{84}$$

and, finally, from the minimization of the total energy (Eq. 82), the equilibrium equation

$$\mathbf{K}\mathbf{D} + \mathbf{Q} = \mathbf{F}. \tag{85}$$

Now the static assumption can be removed allowing the external force $\mathbf{F}$ to vary with time $t \in [0,T]$ where T is the time a moving load needs to cross the beam. Furthermore the connector response $Q_i = Q_i(\mathbf{p}^i, t)$ depends on the local shear slip history $s_i(\tau)$, $\tau \in [0,T]$, through a set of local state parameters $\mathbf{p}^i$. Neglecting inertia and damping forces, equilibrium Eq. (85) reads

$$\mathbf{K}\mathbf{D}(t) + \mathbf{Q}(\mathbf{P}, \mathbf{D}(t)) = \mathbf{F}(t), \tag{86}$$

where $\mathbf{P}$ is the complete set of state parameters of the connectors.

The nonlinear set of Eqs. (86) are solved by the modified Newton Raphson algorithm. Starting from a uniform discretization of the time domain into N time steps of size $\Delta T = T / N$, the algorithm consists in the repetition of the following procedure, until $t_n \geq T$.

Let $t_n = n\Delta T$, $\mathbf{D}^n, \mathbf{P}^n$ be an estimate of $\mathbf{D}(t_n), \mathbf{P}(t_n)$, and $^1\delta\mathbf{F} := \mathbf{F}(t_{n+1}) - \mathbf{F}(t_n)$, $^1\mathbf{D} := \mathbf{D}^n$, solve iteratively for m=1,2,…,the problem:

1) $^1\delta\mathbf{F} := \mathbf{F}(t_{n+1}) - \mathbf{F}(t_n)$,

2) evaluate $\quad ^m\mathbf{S} = \partial\mathbf{Q} / \partial\mathbf{D}(^m\mathbf{D})$,

3) solve $\quad \left[^m\mathbf{S} + \mathbf{K}\right]\delta\mathbf{D} = {}^m\delta\mathbf{F}$,

4) evaluate $\quad ^{m+1}\mathbf{D} = {}^m\mathbf{D} + \delta\mathbf{D}$ and $^{m+1}\delta\mathbf{F} = \mathbf{F}(t_{n+1}) - \mathbf{K}\,^m\mathbf{D} - \mathbf{Q}(^m\mathbf{D})$,

5) evaluate $^{m+1}\varepsilon = \left\|^{m+1}\delta\mathbf{F} - {}^m\delta\mathbf{F}\right\| / \left\|^1\delta\mathbf{F}\right\|$ and return to step 1 if $^{m+1}\varepsilon > \varepsilon_0$,

6) update $\mathbf{D}^{n+1}$ with the last evaluated $^m\mathbf{D}$ and stop the procedure.

In step 5 ε_0 is the required maximum equilibrium error. The rate of convergence of the above procedure is slowed-down, if not broken-down, by very frequent changes in the loading-unloading condition of some connectors, which produces a strong variation in a few components of $^m\mathbf{S}$. To overcome this difficulty, a variable time step strategy was introduced after step 4. Let $\mathbf{u}$ be the subset of $\mathbf{P}$ made by that boolean parameters describing the loading-unloading state of the connectors. If passing from $^m\mathbf{D}$ to $^{m+1}\mathbf{D}$ it produces a change in $\mathbf{u}$, $^{m+1}\mathbf{D}$ is rejected, and the procedure is repeated, keeping the connector state frozen, with an increasingly smaller time step $\Delta T / \alpha$, $\alpha = 10 \div 100$. In Figure 27a, the thick solid line represents the load-slip path of a connector that passing from time t_n (point A) to t_{n+1} (point B) changes its state from a loading to an unloading condition.
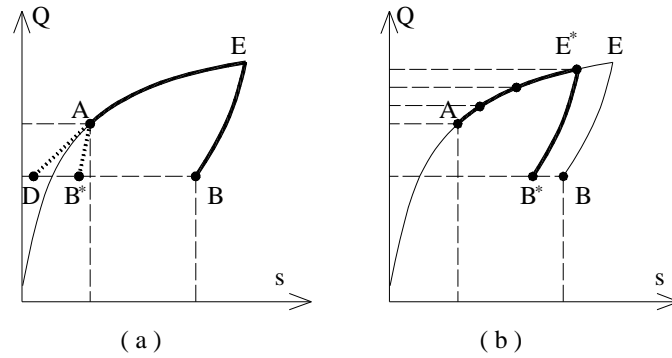
Figure 27 - The variable time step size procedure.

Dotted lines A-D and A-B* represent the path the Newton Raphson procedure would follow without the variable step size strategy depending on the last updated tangent stiffness ^{m}**S**. In Figure 27b the thick line represents the actual path followed by the variable step size procedure. After the trial step of Figure 27a has been performed the procedure assumes a prediction of unloading, freezes the connector in the load state and proceeds with reduced time steps along the curve A-E until a new unloading condition is detected. Then, the system is reset to the last known load (point E*), the connector is unfrozen, the tangent stiffness matrix updated, and the original procedure restarted with the original time step size.

9.3   Fatigue damage

At the end of the structural analysis both the slip and shear force oscillograms of each connector is obtained. It is then possible to evaluate the damage occurred in the connectors due to the cyclic loading pattern considered.

For such a goal it is necessary to adopt one of the methods available for fatigue studies: stress-life approach, strain-life approach or fracture mechanics (Bannantine et al. 1990). The former, which is considered as common method for fatigue checks in most codes of practice, assumes that the endurance depends only on the range of the cyclic load and it is simply needed to compare the acting stress range $\Delta\sigma_A$ with the resistance range $\Delta\sigma_R$, corresponding to the number of cycles considered. The resistance range is given by codes of practice for each detail class (Wöhler curves). For stud connectors the fatigue resistance curve is given by

$$\Delta Q_R = \alpha \cdot N^\beta , \tag{87}$$

where ΔQ_R is the shear force range, N is the number of cycles, β=-0.20 and α, for stud connectors 19 mm diameter, is equal to 413 kN. But the resistance curve described with Eq. (87) can be used only for values of the shear force in the connector not greater than 50% of the monotonic shear capacity (0.5 Q_u) (Mainstone & Menzies 1967).

In bridges the live loads are due to vehicles which are characterized by different weights and axle distances. Some of these vehicles may be very heavy to cause values of the shear load in the connection larger than 0.5 Q_u, so that a different approach, able to consider the actual nonlinear behavior of the connection, is needed to evaluate the damage caused by these cyclic loadings. The approach proposed in Gattesco & Giuriani (1998) considers fatigue resistance curves, in terms of maximum slip and minimum to maximum slip ratio, and the slip

cycles of the connectors are evaluated through a cyclic nonlinear analysis of the structure, as described in the preceding section.
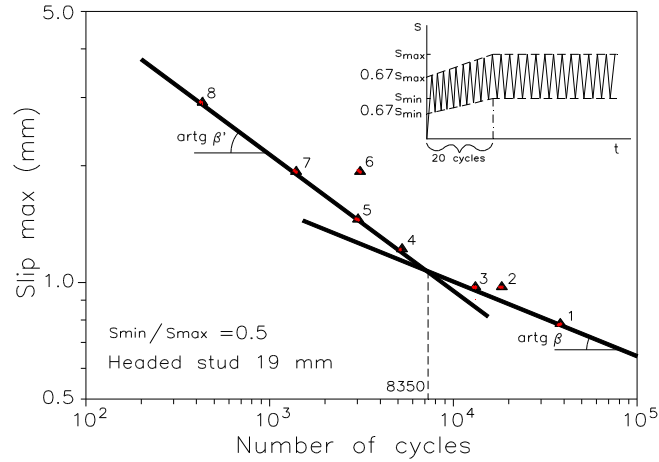

Figure 28 – Maximum slip versus number of cycles at failure: experimental results of Gattesco et al. (1997) (symbols) and theoretical curves (Eq. 88) (solid lines).

The fatigue resistance curve in terms of slip may be represented in a log-log diagram by two straight lines with different slope. The former is steeper and concerns the cases when significant inelastic slip is involved; the latter has a smaller slope and refers to cases when the connector behavior may be assumed as elastic. The intersection of the lines represents the separation between low-cycle and high-cycle fatigue (Fig. 28). The curves are described by the expression

$$s_R = \frac{\gamma}{1-\varepsilon} \cdot N^\beta,$$ (88)

where s_R is the maximum slip, N is the number of cycles, $\gamma/(1-\varepsilon)$ is the intercept on the ordinate axis and ε is the ratio between minimum and maximum slips.

The values of the parameters γ e β were determined from the experimental results of Gattesco et al. (1997), carried out at constant maximum slip and with a minimum to maximum slip ratio equal to 0.5 (Fig. 28). In particular, for the low-cycle fatigue curve $\gamma=11$ mm and $\beta=-0.33$, while for the high-cycle fatigue curve $\gamma=3.3$ mm, $\beta=-0.20$. Actually the number of tests considered is rather limited, but no other experimental results are available, up to now, for low-cycle fatigue; whereas for high cycle fatigue similar values were derived considering also other experimental results available in the literature (e.g. Mainstone & Menzies 1967).

As stated above, bridges are subjected to complex load histories due to the transit of vehicles of different weight. To account for the fatigue damage, it is necessary to identify the cycles with the corresponding maximum slip and minimum to maximum slip ratio. Provided that numerous cycles with different characteristics (s_{max}, s_{min}/s_{max}) can be obtained, the total damage may be determined by summation of the damage due to each block of cycles. Assuming that the damage D_i, due to a block of cycles with same characteristics, is proportional to the ratio between the actual number of cycles n_i and the life to failure N_i for that event (Miner's rule), the total damage is equal to

$$D = \sum_i \frac{n_i}{N_i} \, . \tag{89}$$

This assumption considers that the damage varies linearly with the number of cycles, therefore the sequence of the events (occurrence of blocks of cycles) do not influence the level of damage. The collapse for fatigue occurs when $D=1$.

9.4 Analysis of a bridge girder

The numerical procedure was used to simulate the behavior of a single span simply supported composite bridge (40 m) subjected to a particular model of moving loads, which represent the transit of a non frequent very heavy vehicle (abnormal vehicle in EN 1991-3, 1998). The bridge deck carries a three-lane motorway and has an overall width of 11 meters. Two longitudinal steel girders placed at 5.5 m spacing support a concrete slab, 220 mm depth, connected to them through 19 mm headed stud. The cross section of the bridge girder is illustrated in Fig. 29. Stud connectors were arranged in nine blocks of equally spaced studs (Table 7) designed according to the longitudinal shear caused by the loading model 1 (EN 1991-3 1998).

Table 7. Distribution of stud connectors along half span.

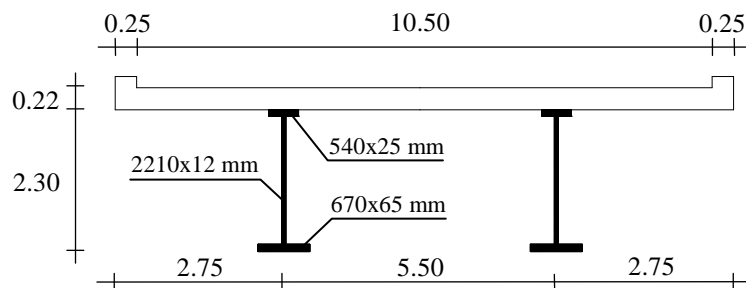| Abscissa [m]	Studs per group	Spacing [mm]
0.00 ÷ 4.00	3	200
4.00 ÷ 10.00	3	250
10.00 ÷ 13.50	2	250
13.50 ÷ 16.50	2	300
16.50 ÷ 20.00	2	350

Figure 29 - Cross section of the bridge girder.
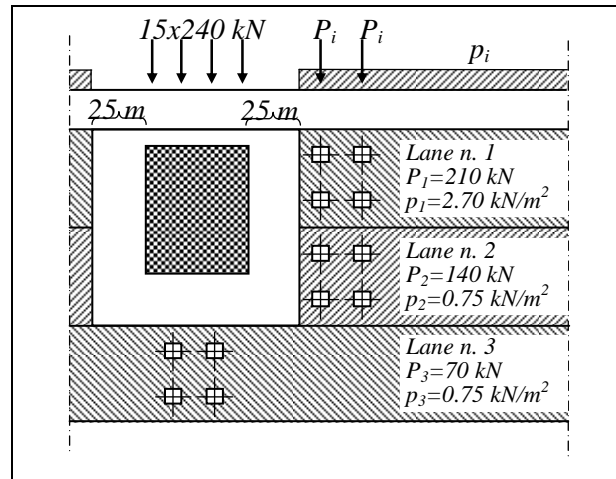*Fatigue model 1 plus a heavy vehicle 3600 kN*

Figure 30. Moving load pattern: fatigue loading model 1 plus a heavy vehicle 3600 kN.

The numerical simulations consider a combination of fatigue loading model 1 and a heavy abnormal vehicle weighting 3600 kN. In particular it consists of a vehicle with 15 axles equally spaced (1.50 m), weighting 240 kN each. In front of and behind such a vehicle, an unloaded zone of 25 m is considered; outside this zone the fatigue loading model 1 is added, as shown in Fig. 30. This type of loading was considered with the main purpose to assess the effect on the shear connection of the occurrence of several very severe loading events on the structure.

The numerical simulation shows that significant slip values are obtained at the interface and the range of the shear force in all connectors is rather large; moreover the maximum shear force is greater than 50% of the stud capacity. In Fig. 31a,b are plotted the oscillograms of the slip near to mid-span (23.15 m far from left support) and close to the right support (40.00 m), respectively, caused by the transit of the loading block illustrated in the top-right window of the figures (40 m p_i, 2 P_i, 25 m unloaded, 15 axles 240 kN). The abscissa axis represents the distance of the loading block from left support (x). The corresponding oscillograms of the shear force are plotted in Fig. 32a,b. Two major cycles occur, at each transit of the loading block, in the connectors near the midspan (Fig. 31a, 32a).

The numerical simulation considers 1000 transits of the loading model (Fig. 30). As evidenced in Fig. 32, this moving load causes, in most connectors of the beam, a shear force larger than 50% of the monotonic shear capacity of the studs, so that the evaluation of the damage due to fatigue needs to follow the strain-life approach. The oscillograms of the slip, evaluated considering the actual cyclic behavior of the connectors, are available from the numerical simulation (Fig. 31). The number and characteristics of each single cycle are determined using the rainflow cycle counting technique. Actually almost all cycles are different one another, however, in order to evidence their characteristics they are grouped in discrete arrays considering five classes for maximum slip and each class has five sub-classes for different values of the slip range. In Table 8 the blocks of cycles belonging to a combination of maximum slip class and slip range sub-class are summarized, for a stud connector near to mid-span (23.15 m). The dimension of maximum slip class and slip range sub-class are 0.075 mm and 0.11, respectively. Each transit of the loading model causes two main cycles of different maximum slip and slip range, so that a number of cycles close to the number of transits is present in two cells of Table 8. In Table 9 the percentage of total damage

due to each combination of maximum slip and slip range classes is reported. It is evident that most of the damage is due to cycles with the higher maximum slip (s_{max}=0.42÷0.495 mm, s_{min}/s_{max}=-0.23÷-0.12).
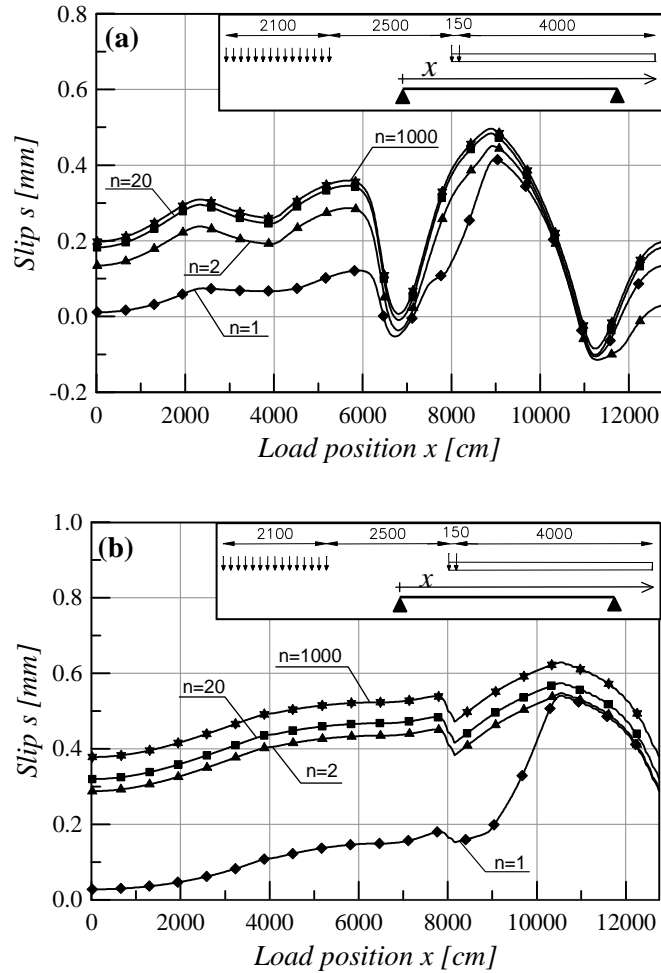
Figure 31 - Oscillograms of the slip: a) near to mid-span (23.15 m); b) close to support (40.00 m).

Using Eq. (88) the life to failure corresponding to each cycle is calculated; the inverse of this number represents the fraction of damage caused by one cycle. The total damage caused by the transit of 1000 times the load configuration of Fig. 30 is obtained through the summation of the damage of each single cycle. The level of damage occurred in a connector near the mid-span (23.15 m) after 1000 transits of the loading model is equal to 16.1% (D=0.161), the damage accumulated in a connector at third span (13.80 m) is equal to 7.54% (D=0.0754), while the damage in a connector close to the support (40.00 m) is equal to 2.5%.

These results evidence that the connectors close to mid-span may reach the collapse for fatigue after several thousands of transits of the loading model considered.

The results show that, except for the first cycle, limited variations of the slip and the shear force at the increase of the number of cycles occur. Actually, a progressive increase of the slip has to be awaited due to the stud stiffness decrement with the damage of the connector shank. The cyclic load-slip relationship of the stud do not include such a damage.
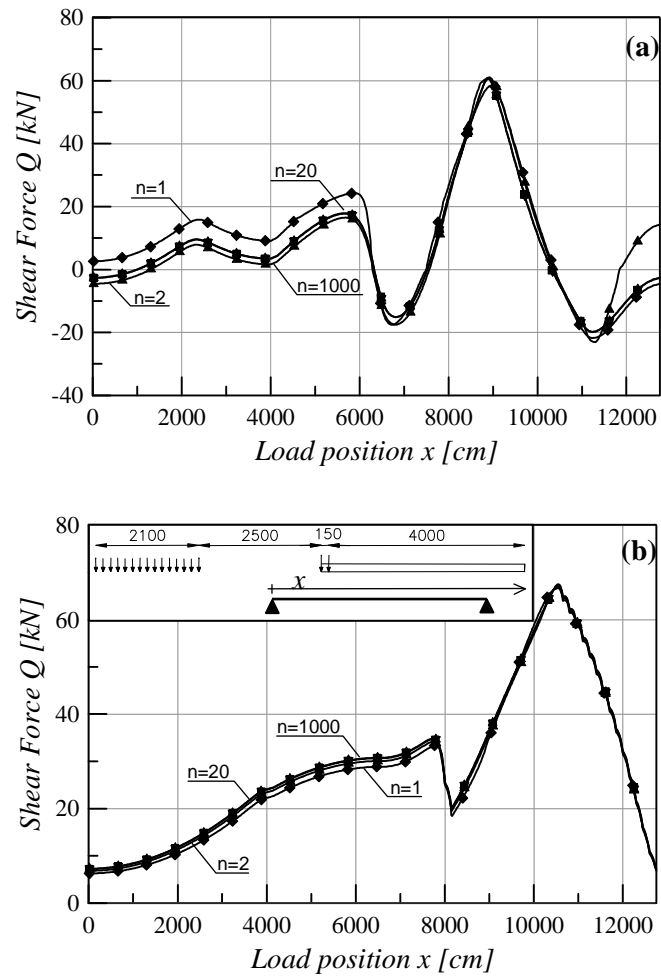
Figure 32 - Oscillograms of stud shear force: a) near to mid-span (23.15 m); b) close to right support (40.00 m).

Table 8 - Number of cycles per each class for a connector near to mid-span (23.15 m), due to 1000 transits of the loading model

Maximum slip class	Slip range class (*class dim. 0.11*)				
(*class dim. 0.075 mm*)	-0.39	-0.28	-0.17	-0.07	0.04
0.160 mm	0	0	0	0	1
0.235 mm	2	1	0	0	0
0.310 mm	0	1	1	17	0
0.385 mm	0	0	1	17	961
0.460 mm	0	4	991	0	0

Table 9 - Percentage of total damage due to the block of cycles of each class for a connector near to mid-span (23.15 m), for 1000 transits of the loading model

Maximum slip class	Slip range class (*class dim. 0.11*)				
(*class dim. 0.075 mm*)	-0.39	-0.28	-0.17	-0.07	0.04
0.160 mm	0.00	0.00	0.00	0.00	0.00
0.235 mm	0.01	0.00	0.00	0.00	0.00
0.310 mm	0.00	0.02	0.01	0.13	0.00
0.385 mm	0.00	0.00	0.04	0.37	12.37
0.460 mm	0.00	0.45	86.59	0.00	0.00

10   Concluding remaks

The main aspects that have to be considered in the analysis of the behavior of composite constructions are evidenced and discussed. In particular, the attention is devoted to continuous composite beams evidencing and facing in depth all the peculiarities that influence the structural behavior both at ultimate and at serviceability limit state level.

An equivalent width of the slab has to be used to evaluate correctly the maximum stresses in the concrete because of the shear lag effect. Moreover steel elements in compression may buckle locally so in the structural analysis this occurrence has to be taken into consideration. To simplify this problem a subdivision of the sections in 4 classes is done.

The expressions of the resistance of sections, both in sagging and hogging moment regions, are presented for the cases when the plastic analysis is possible (class 1 and 2), considering also the influence of a partial shear connection on the resistance of sections subjected to positive bending moment.

For serviceability limit states in all sections and for ultimate limit states in class 3 and 4 sections the elastic analysis has to be adopted. In these cases both the construction method and the time-dependent effects (creep and shrinkage) has to be considered. In the first case the superposition of the effects related to the different phases need to be considered; in the latter the evaluation of creep and shrinkage effects need to be done.

Besides the calculation of stresses in service, assumes great importance the correct evaluation of the deflection and the crack opening. For the calculation of the deflection in continuous beams the procedure has to account for the contribution of tension stiffening of the concrete in tension among two consecutive cracks. Moreover, in case of partial shear connection, the deflection has to be corrected accounting for the slip at steel concrete interface. For evaluating the crack opening, the procedure of reinforced concrete members is used (Eurocode 2-2004).

The global analysis of the structure may be carried out by using linear elastic analysis, rigid-plastic analysis or nonlinear analysis. The moments calculated for ultimate limit states through linear elastic analysis are normally redistributed to account for the inelastic behavior of materials and the cracking of concrete in hogging moment regions. The permissible redistribution values are limited by the ultimate rotation of sections, which are obtained by crushing of concrete in compression, by buckling of steel parts of the steel member or by the attainment of the ultimate uniform strain in the reinforcement.

A broad numerical study permitted to determine a domain of permissible moment redistribution for sections in class 1 taking into consideration both the rotation compatibility (ULS) and the maximum allowable crack opening (SLS). A wide range of sections was considered and two static schemes: propped cantilever and fixed-end beam. The results evidenced that a moment redistribution percentage of 30%, which is the value suggested by the AISC 360-05, can be used when the reinforcement percentage A_r/A_c is greater than 0.875%. Otherwise, a linear relation with zero redistribution, for A_r/A_c=0.5%, and 30%, for A_r/A_c=0.875%, should be employed to limit the concrete cracking ($w_k \leq 0.3$ mm).

It is also presented a numerical procedure able to simulate the actual behavior of bridge type composite girders subjected to moving loads, based on a special finite element made by two unidimensional elements connected at the ends by two nonlinear springs, which simulate stud connectors.

The fatigue analysis of the connection under the most severe moving loads can be carried out using the strain-life approach, in order to account for significant nonlinear deformations of the connectors. The numerical procedure allows evaluating correctly the actual slip oscillograms of the connectors per each transit of the loading model considered. From the oscillograms the number and characteristics of cycles are derived by means of the rainflow technique. In the hypothesis of damage varying linearly with the number of cycles (Miner's rule) and considering the slip-life curve proposed in Gattesco and Giuriani (1998), the fatigue damage caused by an assigned sequence of loading models can be calculated.

The numerical simulation of the behavior of a simply supported bridge composite girder with a 40 m span subjected to a severe cyclic loading, fatigue model 1 of ENV 1991-3 (1998) and heavy abnormal 15 axles vehicle (3600 kN), was carried out. The results show that both slip and shear force are large enough to cause a possible stud collapse after a few thousands of cycles. In fact the damage accumulated, after 1000 transits of the loading model considered, is 16% in the studs near the mid-span.

Further experimental fatigue tests on stud connectors between two fixed values of the slip need to be carried out so to confirm the validity of the slip-life curve proposed for low-cycle fatigue. Moreover different sequences of actual commercial vehicles need to be considered so to evaluate the response of the structure to a true loading history.

11   References

[1]   AISC 360-05 (2005). "Specification for Structural Steel Buildings", American Institute of Steel Construction, Inc., Chicago, Illinois, U.S.A.

[2]   Aribert J. M., Aziz K. A., (1986) "Modèle Général pour le Calcul des Poutres Mixtes Hypertatiques jusqu'à la Ruine", *Construction Métallique*, No. 4, pp. 3-41.

[3]   Bannantine, J.A., Comer, J.J. and Handrock, J.L. (1990), "Fundamentals of Metal Fatigue Analysis", Prentice Hall, Englewood Cliffs, New Jersey 07632.

[4]   Beeby, A. W. (1998). "Tests to investigate the influence of reinforcement parameters on rotation capacity." *CEB Bulletin d'Information No. 242*, Lausanne, Switzerland, 309-323.

[5]   Bigaj-van Vliet, A., and Mayer, U. (1998). "Round robin analysis of available rotation capacity of plastic hinges – evaluation." *CEB Bulletin d'Information No. 242*, Lausanne, Switzerland, 143-156.

[6]   CEB (1993). "CEB-FIP Model Code 90." *CEB Bull. No. 213/214*, Lausanne, Switzerland.

[7]   CEB-FIP, 1990, *Evaluation of Time Dependent Behavior of Concrete*, Bull. No. 199.

[8]   Chapman J. C., Balakrishnan S., (1964), "Experiments on Composite Beams", *The Structural Engineer*, 42, pp. 369-383.

[9]   Cosenza, E., Greco, C., and Manfredi, G.. (1993). "The concept of equivalent steel.", *CEB Bulletin d'Information No. 218*, Lausanne, Switzerland, 163-184.

[10]   Dezi L., Gattesco N., (2006), *Composite Structures – New Buildings, Restoration, Bridges,* CISM Press, Udine, Italy.

[11]   Dezi, L., Leoni, G., and Tarantino, A. M. (1995). "Time-dependent analysis of prestressed composite beams." *Journal of Structural Engineering*, ASCE, 121(4), 621-633.

[12]   Eurocode 2, 2004, *Design of concrete structures - Part 1-1: General rules and rules for buildings, EN 1992-2004,* CEN/TC 250, Brussels, Belgium.

[13]   Eurocode 3, (2005), *Design of steel structures - Part 1-1: General rules and rules for buildings, EN 1993-2005,* CEN/TC 250, Brussels, Belgium.

[14]   Eurocode 4, (2004), *Design of Composite Steel and Concrete Structures – Part 1-1: General and Common Rules for Buildings, EN 1994-2004,* CEN/TC 250, Brussels, Belgium.

[15]   Fabbrocino, G., Manfredi, G., Cosenza E., (1998). "Rotation capacity of steel-concrete composite beams: influence of reinforcing steel properties.", *Costruzioni Metalliche*, 6, 43-50 (in Italian).

[16]   Fragiacomo, M., Amadio, C., and Macorini, L. (2004). "A finite element model for collapse and long-term analysis of steel-concrete composite beams." *J. Struct. Engrg. ASCE*, 130(3), 489-497.

[17]   Gattesco, N. (1997), "Fatigue in Stud Shear Connectors". *Int. Conf. 'Composite Construction – Conventional and Innovative*, Innsbruck, Austria, 139-144.

[18]   Gattesco, N. (1999). "Analytical modeling of nonlinear behavior of composite beams with deformable connection." *J. Construct. Steel Research*, 52(2), 195-218.

[19]   Gattesco, N., and Cohn, M.Z. (1989). "Computer-simulated tests on moment redistribution. Part I: ULS consideration." *Studi e Ricerche, F.lli Pesenti, Politecnico di Milano,*11, 269-299.

[20]   Gattesco, N., and Gasparotto, S. (2003). "Moment redistribution in steel-concrete composite beams." *2ⁿᵈ Int. Spec. Conf. 'The conceptual approach to struct. design'*, Milano (Italy), Vol. 2, 459-466.

[21]   Gattesco, N. and Giuriani, E. (1996). "Experimental Study on Stud Shear Connectors Subjected to Cyclic Loading". *J. of Constr. Steel Res.*, Vol. 38(1), 1-21.

[22]   Gattesco, N., Giuriani, E. and Gubana, A. (1997), "Low-Cycle Fatigue Tests on Stud Shear Connectors". *J. Struct. Engrg. ASCE*, Vol. 123(2), 145-150.

[23]   Gattesco, N. and Giuriani, E. (1998), "The Problem of Low-Cycle Fatigue in Stud Shear Connections: Damage Cumulativeness Considerations", *III Workshop Italiano sulle Strutture Composte,* Ancona, 201-210.

[24]   Gattesco N., Macorini L., Fragiacomo M., (2010), "Moment Redistribution in Continuous Steel-Concrete Composite Beams with Compact Cross Section", *ASCE, Journal of Structural Engineering*, Vol. 136, No. 2, Feb., pp. 193-202.

[25]   Gattesco N., Pitacco I., (2004), "Analysis of the Cyclic Behavior of Shear Connections in Steel-Concrete Composite Bridge Beams due to Moving Loads", *Proc. 2° Int. Conf. on Steel and Composite Structures, ICSCS 04*, 2-4 Sept., Seoul, Korea.

[26]   Gattesco, N. and Rigo, G. (1999), "Stud Shear Connections in Steel and Concrete Composite Beams: Experimental Investigation of The Behavior Under Cyclic Loads". *Pers. comm.*

[27]   Gilbert, R. I., and Bradford, M. A. (1995). "Time-dependent behavior of continuous composite beams at service load." *Journal of Structural Engineering*, ASCE, 121(2), 319-327.

[28] Johnson R.P., (1994), *Composite Structures of Steel and Concrete, Volume 1: Beams, Slabs, Columns and Frames for Buildings,* Blackwell Scientific Publications, Oxford, U.K.

[29] Johnson R.P., Buckby R.J., (1994), *Composite Structures of Steel and Concrete, Volume 2: Bridges,* Blackwell Scientific Publications, Oxford, U.K.

[30] Johnson, R.P., and May, I.M. (1975). "Partial-interaction design of composite beams." *The Struct. Eng.*, 53(8), 305-311.

[31] Kemp, A.R. (1985). "Interaction of plastic local and lateral buckling." *Journal of Structural Engineering*, *ASCE*, 111(10), 2181-2196.

[32] Kemp, A.R. (1986). "Factors affecting the rotation capacity of plastically-designed members." *The Structural Engineer*, 64B(2), 28-35.

[33] Kemp, A.R., and Dekker, N.W. (1991). "Available rotation capacity in steel and composite beams." *The Structural Engineer*, 69(5), 88-97.

[34] Kemp, A.R., and Nethercot, D.A. (2001). "Required and available rotations in continuous composite beams with semi-rigid connections". *J. Construct. Steel Research*, 57, 375-400.

[35] Kristek V., Evans H.R., Ahmad M.K.M., (1990), "A Shear-Lag Analysis for Composite Box Girders", *J. Constr. Steel Research*, Vol. 16, pp. 1-21.

[36] Kristek V., and Studnicka J., (1982), "Analysis of Composite Girders with Deformable Connectors", *ICE Proceedings*, Vol. 73, No. 4, pp. 699-712.

[37] Lukey, A. F., and Adams, P. R. (1969). "Rotation capacity of wide-flange beams under moment gradient." *Journal of the Structural Division, ASCE,* 95(ST6), 1173-1188.

[38] Macorini, L., Fragiacomo, M., Amadio, C., and Izzuddin, B.A. (2006). "Long term analysis of steel-concrete composite beams: FE modelling for effective width evaluation." *Engineering Structures*, 28(8), 1110-1121.

[39] Mainstone, R.J. and Menzies, J.B. (1967), "Shear Connectors in Steel-Concrete Composite Beams for Bridges. Part 1: Static and Fatigue Tests on Push-out Specimens", *Concrete*, Vol. 1(9), 291-302.

[40] Mander, J.B., Priestley, M.J.N., and Park, R. (1988). "Theoretical stress strain model for confined concrete." *J. Struct. Engrg.*, 114(8), 1804-1826.

[41] Ollgard, J.G., Slutter, R.G., and Fisher, J.W. (1971). "Shear strength of stud connectors in lightweight and normal weight concrete." *AISC Engineering Journal*, 55-64.

[42] Salari, M. R., Spacone, E., Shing, P. B., and Frangopol, D.M. (1998). "Nonlinear analysis of composite beams with deformable shear connectors." *Journal of Structural Engineering*, *ASCE*, 124(10), 1148-1158.

[43] Teraszkiewicz J. S., (1967), "Static and Fatigue Behavior of Simply Supported and Continuous Composite Beams of Steel and Concrete.", *PhD thesis*, University of London.

12   Curriculum Vitae

Doc. Dott.-Ing. Natalino Gattesco

Born: Dec. 16, 1958, Mortegliano, Udine, Italy.

Education and scientific degrees:

Sept. 1989 to March 1990   Mc Master University, Hamilton, Ontario (Canada)
Design of Reinforced Concrete Buildings in Seismic Zones. *Specialty Course held by Prof. Tom Paulay, Canterbury University, New Zealand.*

Oct. 1977 to March 1983   Faculty of Engineering, University of Udine (Italy)
Civil Engineering "Laurea" Dottore in Ingegneria Civile - Thesis: Effects of creep in reinforced concrete structures.

Other titles:

2010-present   Member of the Evaluation Board of research projects subjected to grant in Italy (FIRB projects), Ministry of Education, University and Research (MIUR)

2008-present   Member of the Structural Timber Committee of the Italian Organization for Standardization UNI.

2005-present   Member of the Structural Timber Committee of the Italian Council of Research CNR.

2003-2006   President of the Structural Committee of the Federation of Professional Engineers of Friuli Venezia Giulia Region, Italy.

2002-present   Member of the Evaluation Board of research projects subjected to grant in Czech Republic, GACR (Grant Agency of the Czech Republic)

2002-present   Member of the Evaluation Board of research projects subjected to grant in Italy, Ministry of Education, University and Research (MIUR)

2002-2009   President of the Structural Committee of the Professional Engineer Association of the Province of Udine, Italy.

2000-present   Member of the Technical Consulting Board of the Court of Justice in Udine, Italy.

1994-present   Member of the Inspection Board of the Friuli Venezia Giulia Region for Engineering structures built in seismic zones

1983-present   Member of the Professional Engineer Association of the Province of Udine, Italy,

June 1983   Professional Engineer Licence – Technical University of Milan (Italy).

Professional career :

Apr. 2011
  Associate Professor on Structural Engineering, Czech Technical University, Prague.

Apr. 2008 – up to now.
  Member of the Lecturer Board; PhD Program on "Rehabilitation of ancient and modern buildings", offered by the partnership of the Universities of Brescia, Padova, Trento, Trieste, Udine, Venezia; lead partner Brescia.

Oct. 2007 – up to now.

Member of the Lecturer Board; Master Program on "Structural Design in Seismic Areas", offered by the University of Trieste.

Nov. 2001 – up to now.

Associate Professor of Structural Engineering, in charge to teach Structural Mechanics, Structural Behavior of Ancient Buildings, Masonry and Timber Structures; Faculty of Architecture, University of Trieste.

Nov. 2000 – up to now.

Member of the Lecturer Board; PhD Program on "Engineering of Civil and Mechanical Structural Systems", offered by the partnership of the Universities of Brescia, Padova, Trento, Trieste, Udine, Venezia; lead partner University of Trento.

Jul. 1986 – Oct. 2001.

Assistant Professor; entrusted to research in the field of Structural Engineering and to take lectures and/or exercises in courses belonging to the same field; Department of Civil Engineering, University of Udine, Italy.

Jul. 1986 – Oct. 2001, (except from March 1989 to May 1990).

Laboratory expert supervisor; as Assistant Professor was also entrusted to supervise the development both in equipment and services of the Laboratory for Testing Materials and Structures of the Department of Civil Engineering, University of Udine, Italy.

Jun. 1992 – Jul. 1992.

Visiting Scholar; involved in study and research on steel-concrete composite structures at the University of Warwick, Coventry, UK, invited by Prof. R.P. Johnson.

March 1989 - May 1990.

Visiting Scholar; involved in research on nonlinear analysis of concrete structures at the University of Waterloo, Waterloo, Ontario (Canada), invited by prof. M. Z. Cohn.

May 1989.

Award; won a one year C.N.R. - N.A.T.O. fellowship spent at the Solid Mechanics Division of the University of Waterloo, Waterloo, Ontario (Canada).

Jul. 1985 - Jun. 1986

Laboratory expert technician; entrusted to start and manage the activity of the Laboratory for Testing Materials and Structures of the Institute of Theoretical and Applied Mechanics. One year contract with the University of Udine, Italy.

Oct. 1984 - Jun. 1985

Research associate; Institute of Theoretical and Applied Mechanics of the University of Udine, involved in research on concrete structures under the direction of prof. Giandomenico Toniolo (full professor of Structural Design).

Oct. 1983 - Sept. 1984

Research fellow; Institute of Theoretical and Applied Mechanics of the University of Udine – involved in research on the nonlinear behavior of concrete structures under the direction of prof. Giandomenico Toniolo.

Oct. 1983

Award; won a one year fellowship offered by the Industrial Association of the Province of Udine; spent in carrying out research at the Institute of Theoretical and Applied Mechanics of the University of Udine.

Jul. 1983 – up to now.

Consulting engineer; besides the academic activity various structural designs of concrete and steel buildings, or special constructions, were carried out as self-governing professional engineer.

<u>Scientific Associations Memberships:</u>

1986-present   Member of the Association for the Industrialization of Buildings CTE, Italy.

2006-present   Member of the National Association for Earthquake Engineering ANIDIS, Italy.

2005-present   Member of the Structural Timber Committee of the Italian Council of Research CNR.

<u>Research activity :</u>

The main fields of research are the following:
- Theoretical and numerical modeling of structural behavior
- Structural analysis
- Nonlinear analysis of structures (concrete, composite, etc.)
- Fatigue in steel concrete composite bridges
- Time-dependent behavior of concrete structures
- Testing methods in civil engineering
- Monitoring of structures
- Diagnostics of structures.
- Mechanical joints in timber structures.
- Strengthening of ancient wooden floors.
- Rehabilitation techniques for existing masonry structures
- Durability of concrete structures
- Earthquake engineering
- Seismic vulnerability of existing constructions

The research is normally carried out with the purpose of understanding the local or global structural behavior through specific experimental investigations, which allowed setting up numerical and/or analytical models able to simulate the actual behavior.

Specifically in the research activity the following projects may be evidenced:

1. steel-concrete composite structures: cyclic loads, nonlinear behavior, diagnostics;
2. strengthening and stiffening of wooden floors and masonry walls to improve the resistance of ancient masonry buildings to earthquakes;
3. experimental and numerical investigation on the behavior of mechanical joints in glued laminated timber structures;
4. nonlinear analysis of concrete structures concerning both normal and high performance concrete;
5. effects of creep on the behavior of concrete structures;

<u>Research projects granted by Public Institutions</u>.

The applicant partecipated in the following research projects either as coordinator or as member of the research group.
- "Innovative techniques and numerical models for the design of reinforced and prestressed concrete structures". Coordinated by Prof. Pier Giorgio Malerba. Project financed by the Italian Ministry of University and Research (MIUR) – 1995.
- "Resisting mechanisms, cracking, damage and corrosion in NSC and HSC structures". Coordinated by Prof. Pier Giorgio Malerba. Project financed by the Italian Ministry of University and Research (MIUR) – 1996.

- "HSC Benefits on durability behavior of reinforced and prestressed concrete elements made with high strength concrete". Coordinated by Prof. Pier Giorgio Malerba. Project financed by the Italian Ministry of University and Research (MIUR) – 1997.
- "Providing new didactic tools to teach structural analysis according to the new university schedules". Coordinated by Prof. Pier Giorgio Malerba. Financed by the Friuli Venezia Giulia Region, Italy – 2000.
- "Durability and reliability analyses on reinforced and prestressed concrete structures with or without damage". Coordinated by Prof. Pier Giorgio Malerba/Prof. Gaetano Russo. Project financed by the Italian Ministry of University and Research (MIUR) – 2000.
- "Innovative connection techniques for timber members: experimental investigation to define connection characterized by effectiveness even with cyclic loads, easyness to apply and good esthetic aspect". Coordinated by the applicant. Financed by the Friuli Venezia Giulia Region, the firm Stratex S.p.A., Sutrio, Udine and the enterprise Plus s.r.l., Cassacco, Udine – 2002.
- "Inverse problems in structural diagnostics: general aspects and applications". Coordinated by Prof. Antonino Morassi. Project financed by the Italian Ministry of University and Research (MIUR) – 2003.
- "Assessment and reduction of the seismic vulnerability of masonry buildings". Coordinated locally by the applicant. National coordinators Proff. Sergio Lagomarsino and Guido Magenes. Financed by the European Community and the National Department of the Civil Protection – 2005-2007 RELUIS.
- "Study of high reversibility techniques for strengthening and stiffening of wooden floors of ancient buildings". Involved five Italian Universities: Bologna, Napoli I, Napoli II, Trento, Trieste. The Unit of Trieste was coordinated by the applicant. Project financed by the Italian Ministry of University and Research (MIUR) – 2006.
- "Analysis of the seismic scenarios concerning the educational buildings aimed to the definition of an intervention priority so to reduce the seismic risk". Structural group coordinated by the applicant. Involved in the project the Universities of Trieste, Udine and the Experimental Geophisic Observatory of Trieste (OGS) – 2008-2010. (ASSESS Project), financed by the Friuli Venezia Giulia Italian Region.
- "Study of new intervention techniques to improve the seismic resistance of the ancient buildings of the Province of Trieste by using innovative materials". Coordinated by Prof. Claudio Amadio. Financed by the Province of Trieste – 2009-2010.
- "Assessment of the seismic vulnerability of masonry buildings, historical centers, cultural heritage". Coordinated locally by the applicant. National coordinators Proff. Sergio Lagomarsino, Claudio Modena and Guido Magenes. Financed by the European Community and the National Department of the Civil Protection – 2010-2012 RELUIS.
- "Innovation in codes and technology concerning seismic engineering. Timber structures.". Coordinated locally by the applicant. National coordinator Prof. Paolo Zanon. Financed by the European Community and the National Department of the Civil Protection – 2010-2012 RELUIS.

Requests of financing research projects proposals to Public Institutions in progress.

The financing of the following project proposals were requested to public institutions:
- "Compatible Materials and Techniques for Protecting Historical Masonry Bridges MATEMA". Seventh Framework Program Proposal by five Universities (Imperial College London UK, CTU Prague CZ, Salerno IT, Trieste IT, Bremen D), two research centers (ZAG Ljubliana SLO, EMPA Zurich CH), six enterprises (FibreNet Udine IT, Maurer Soehne Engineering D, Boviar S.r.l. IT, SM7 a.s. CZ, S&P Clever Reinforcement CH, MaterialTeknic am bau CH). The project leader for the Unit of Trieste is the Applicant. (November 2010).

- "Strategies for the assessment and reduction of seismic risk of existing reinforced concrete buildings in the Friuli Venezia Giulia and Goriska Regions through innovative techniques - VALRICA". INTERREG European Project for Italy and Slovenia. Involves four Institutions: Universities of Trieste and Udine (Italy), ZAG National Research Institution Ljubljana and RRA Regional Research Agency Nova Gorica (Slovenia). The lead partner is the University of Trieste and the team manager is the Applicant (May 2011).

International cooperations

- Prof. Miha Z. Cohn, University of Waterloo, Ontario, Canada. Cooperation in research on the moment redistribution on reinforced concrete frames. 15 months visiting professor at the University of Waterloo (1989-1990).
- Prof. R.P. Johnson, University of Warwick, Coventry, UK. Cooperation in research on the cyclic behavior of steel-concrete composite structures. Two months visisting scholar at the University of Warwick (1992).
- Prof. Miha Tomazevic, ZAG Ljubljana, SLO. Member of the Lecturers Board of the Master Program in Earthquake Engineering of the University of Trieste.
- Prof. Miha Tomazevic and Dr. Marjana Lutman, ZAG Ljubljana, SLO. Cooperation in a pending across border Italy-Slovenia research project dealing with the development of new strategies to assess the structural vulnerability of ancient masonry buildings located in seismic prone areas and to reduce the seismic risk - VALRICA.
- Prof. Vladimir Kristek, Prof. Alena Kohoutkova, Dr. Lukas Vrablik, Czech Technical University of Prague, CZ. Cooperation in a pending FP7 EU Research Project proposal dealing with "Compatible Materials and Techniques for Protecting Historical Masonry Bridges – MATEMA". In 2007 it was signed a research agreement between the Department of Concrete and Masonry Structures of the CTU Prague and the Department of Civil and Environmental Engineering of the University of Trieste. Moreover, Prof. Kristek was invited to take short courses and seminars at the Faculty of Engineering at the University of Trieste.
- Prof. Bassam Izzuddin, Dr. Macorini, Imperial College London, UK. Cooperation in a pending FP7 EU Research Project proposal dealing with "Compatible Materials and Techniques for Protecting Historical Masonry Bridges – MATEMA".
- Prof. Lucio Colombi Ciacchi, University of Bremen, D. Cooperation in a pending FP7 EU Research Project proposal dealing with "Compatible Materials and Techniques for Protecting Historical Masonry Bridges – MATEMA".

Industrial partners supporting research projects

- Stratex S.p.a., via Peschiera, 3/5, Sutrio, Udine, Italy – Industry of Glued Laminated Timber Structures – Financed various research projects aimed to study the behavior of joints in timber structures. (Research projects 2002-2004, 2010-2011 financed by Stratex and the Region Friuli Venezia-Giulia).
- Euroholz s.r.l., via Divisione Julia, Villa Santina, Udine, Italy – Industry of Glued Laminated Timber Structures – Financed various research projects aimed to study the behavior of joints in timber structures.
- Plus S.r.l., viale Udine, 8, Cassacco, Udine, Italy. – Building enterprise of timber dwellings – (Research project 2002-2004 financed by Plus and the Region Friuli Venezia-Giulia aimed to study the behavior of wooden panels when subjected to shear).
- Cimolai Costruzioni Metalliche, viale Venezia, Pordenone, Italy – Industry of Steel Structures – Partly financed research on steel-concrete shear connection.
- Precast S.p.a., via Martiri della Libertà, 12, Sedegliano, Udine. – Agreement for a study concerning the non-destructive testing techniques for concrete structures (2006).

- Spav Prefabbricati S.p.a., via Spilimbergo, 231, Martignacco, Udine, Italy – Industry of Prefabricated Concrete Structures – Financed a research project on the study of multistorey buildings subjected to earthquake (2006-2008).
- Fibre Net s.r.l., via Zanussi, 311, Udine, Italy – Industry of Glass Fibre Polymeric Products – Financed a research project aimed to study the effectiveness of a strengthening technique for existing masonry walls by using GFRP meshes (2008 – in progress).
- MEP S.p.a., via Leonardo Da Vinci, 20, Reana del Roiale, Udine, Italy – Industry producing electronic wire bending machines – It is in progress an agreement for studying an adequate shape for stirrups in reinforced concrete elements that can optimize the time of production and installation.

Teaching and student training activity

- Involved in teaching in the field of structural engineering at the University of Udine, Italy, (1984-2002) and at the University of Trieste, Italy (1999-present). In particular the teaching activity concerned the courses of Structural Design, Theory of Steel Structures, Computational Mechanics, Structural Mechanics, Structural Analysis, Timber and Masonry Structures, Structural Behavior of Ancient Buildings.
- Lectures on specialistic topics (seismic vulnerability of buildings, strengthening techniques, structural behavior of reinforced concrete tanks) in the two Master and two PhD programs of the University of Trieste, Italy.
- Lectures to specialistic topics of the structural engineering for Advanced Professional Training at The International Center of Mechanical Sciences (CISM), Udine, Italy or for Professional Engineer Associations in Italy.
- Supervisor of 38 Laurea Theses, for the degree of Civil Engineer, and 21 Laurea Theses, for the degree of Architecture.
- Supervisor of 10 Master Theses and 2 PhD Theses.

Consulting activity, technical or architectural realizations

In the consulting activity many structural analyses and design on special constructions and many assessments of the seismic vulnerability of important ancient masonry buildings were carried out. Various technical advices were given for the strenthening procedure of both masonry and reinforced concrete structures. Five technical advices were given for the Court of Justice and six expert opinions concerning structural problems of buildings were given in justice procedures.

Publications

13 papers in International Journal with "Impact Factor", 4 papers in International Journal with "review board", 10 papers in Italian Journals or scientific series with "review board", 1 book, 9 parts of books, 28 papers in the proceedings of International Conferences, 42 papers in the proceedings of Italian Conferences, 10 scientific reports, 18 reports of specialistic courses, 11 reports to technical studies, 10 reports of seminars. 105 international citations of main papers, h-index 4.